Recognition and Cleavage of Related to Ubiquitin 1 (Rub1) and Rub1-Ubiquitin Chains by Components of the Ubiquitin-Proteasome System*⑤

Rajesh K. Singh‡, Sylvia Zerath§, Oded Kleifeld¶, Martin Scheffner‖, Michael H. Glickman§, and David Fushman‡**

Of all ubiquitin-like proteins, Rub1 (Nedd8 in mammals) is the closest kin of ubiquitin. We show via NMR that structurally, Rub1 and ubiquitin are fundamentally similar as well. Despite these profound similarities, the prevalence of Rub1/Nedd8 and of ubiquitin as modifiers of the proteome is starkly different, and their attachments to specific substrates perform different functions. Recently, some proteins, including p53, p73, EGFR, caspase-7, and Parkin, have been shown to be modified by both Rub1/Nedd8 and ubiquitin within cells. To understand whether and how it might be possible to distinguish among the same target protein modified by Rub1 or ubiquitin or both, we examined whether ubiquitin receptors can differentiate between Rub1 and ubiquitin. Surprisingly, Rub1 interacts with proteasome ubiquitin-shuttle proteins comparably to ubiquitin but binds more weakly to a proteasomal ubiquitin receptor Rpn10. We identified Rub1-ubiquitin heteromers in yeast and Nedd8-Ub heteromers in human cells. We validate that in human cells and *in vitro*, human Rub1 (Nedd8) forms chains with ubiquitin where it acts as a chain terminator. Interestingly, enzymatically assembled K48-linked Rub1-ubiquitin heterodimers are recognized by various proteasomal ubiquitin shuttles and receptors comparably to K48-linked ubiquitin homodimers. Furthermore, these heterologous chains are cleaved by COP9 signalosome or 26S proteasome. A derubylation function of the proteasome expands the repertoire of its enzymatic activities. In contrast, Rub1 conjugates may be somewhat resilient to the actions of other canonical deubiquitinating enzymes. Taken together, these findings suggest that once Rub1/Nedd8 is channeled into ubiquitin pathways, it is recognized essentially like ubiquitin.

The selective degradation of many proteins in eukaryotic cells is a highly specific and irreversible process required to perform vital cellular functions such as cell cycle progression (1, 2), differentiation and development (3, 4), and transcriptional control (5). One of the major pathways involved in this selective degradation is the ubiquitin-proteasome pathway. In this pathway, ubiquitin (Ub), a 76-amino-acid protein, is attached to the substrate, and this is followed by the recognition and degradation of the substrate by a protein complex collectively known as proteasome (6–8).

The attachment of Ub (ubiquitination) to a substrate protein is achieved via a cascade of enzymatic reactions (involving E1, E2, and E3 enzymes) that results in the formation of an isopeptide bond between the C-terminal glycine of Ub and a lysine residue of the substrate (9–11). Sequential repetition of this cascade can result in the attachment of a chain of Ub molecules (polyubiquitin) to the substrate protein. The length and topology of the polyubiquitin (polyUb) tag decide the fate of the substrate protein. For example, we and others have shown that a K48-linked tetraubiquitin (tetraUb) chain that acts as a proteasomal degradation signal forms a "closed" structure (12, 13), whereas a K63-linked Ub chain forms an "extended " structure (14) and has been implicated in non-proteolytic functions including ribosomal functioning (15, 16) and post-replicational DNA repair (17, 18).

Yeast protein Rub1 and its mammalian orthologue Nedd8 (for simplicity, we refer to the molecule as Rub1 regardless of its source unless specifically highlighting a unique property of the mammalian orthologue, in which case we prefer the name Nedd8), also a 76-amino-acid-long polypeptide, are the closest kin of Ub in the family of Ub-like proteins. Rub1 is ~53% identical and ~77% similar to Ub at the amino acid level. The structures are incredibly similar as well, as the three-dimensional folds of Rub1 orthologues from mammals or plants are largely superimposable with Ub (19–21). Key residues are conserved as well (Fig. 1*A*), suggesting that the overall surface and

functional residues are maintained. Despite these striking similarities, Rub1/Nedd8 and Ub employ their own cognate E1 and E2 to post-translationally modify their specific substrates (22, 23). The recognition of the cognate E2s by their respective E1 paralogues is critical in avoiding cross-talk between these two parallel regulatory pathways (24, 25). The Ub pathway involves the attachment of monomeric Ub or polyUb chains to substrates and has been implicated in degradative and regulatory or protein sorting/trafficking functions. In contrast, the Rub1 pathway exclusively attaches monomeric Rub1 to substrates and performs mainly regulatory functions (26). The attachment of Rub1 (rubylation) to cullin proteins and the subsequent regulation of a multi-subunit E3 ligase, the Skp, cullin, and F-box containing complex, is probably the most prevalent, and clearly the best studied, biological function reported so far (22, 23, 27, 28). However, some other proteins have recently been shown to be modified by Nedd8, including p53 and its E3 ligase Mdm2 (29–31), p73 (a homolog of p53) (32), ribosomal protein L11 (33, 34), epidermal growth factor receptor (EGFR) (35), caspase-7 (36, 37), and parkin (38, 39), though the effects are still vague, particularly as the ratio of modified to unmodified forms of each protein is extremely low. Complicating matters, many of these proteins are also reported to be targets for ubiquitination, and in many cases the same E3 enzymes are required for both ubiquitination and rubylation. Moreover, under certain stress conditions, such as those that occur when the level of free Ub is limiting in cells, the extent of neddylation increases dramatically, in some cases resulting in Rub1/Nedd8 and Ub on the same target (40, 41). This raises the important yet unaddressed question of how the proteasomal and the non-proteasomal Ub receptors differentiate among the same target proteins modified by either Ub or Rub1 or both. To address this question, we examined the interactions of Rub1 with the Ub-binding domains of these receptors. Surprisingly, Rub1 showed binding to all the non-proteasomal receptors/shuttles tested. However, it interacts weakly with a proteasomal Ub-receptor, Rpn10. As these receptors are well known for their preference for Ub chains (42), we tested the ability of human Rub1 (Nedd8) to form chains in H1299 cells. Interestingly, Nedd8 forms a heterologous chain with Ub. Our analysis revealed that in the substrate-free Nedd8-Ub heterodimers, Nedd8 acts as a chain terminator. Moreover, we were able to synthesize these heterodimers *in vitro* using the E1 and E2 enzymes from the Ub pathway. Here we also show that a K48-linked Rub1-Ub heterodimer is recognized by the proteasomal and non-proteasomal Ub-receptors comparably to K48-linked Ub homodimer and is cleaved *in vitro* by either purified 26S proteasome or the COP9 signalosome.

EXPERIMENTAL PROCEDURES

Expression Constructs—The DNA encoding 1–76 amino acids of Rub1 was cloned into pTXB1 vector (NEB) using standard techniques, and the construct was verified by DNA sequencing. Details of the cloning procedure and primer sequences are provided in the supplemental information. All constructs used in this study are listed in supplemental Table S1.

Protein Expression and Purification—All proteins used in this study were expressed in the BL21 (DE3) strain of *E. coli* except for Ub constructs, which were expressed in the pJY2 strain. Proteins were purified using standard chromatographic techniques (see supplemental Table S2).

Synthesis and Purification of Rub1-Ub Dimer—Purified Rub1 and Ub monomers (100 μM each) were incubated with 500 nM of E1 of Ub, 20 μM of E2–25K (or 20 μM each of Ubc13 and Mms2), 5 mM ATP, 5 mM MgCl$_2$, phosphocreatin, and phosphocreatine kinase in 50 mM Tris-HCl buffer (pH 8) for 16 h. Rub1-Ub dimer fractions were purified via gel filtration chromatography. The ^{15}N-labeled Rub1-Ub heterodimer for NMR studies was assembled from ^{15}N-enriched Rub1 and ^{15}N-enriched Ub monomers using the same procedure. After purification, the protein was exchanged into 20 mM phosphate buffer (pH 6.8) containing 0.02% (v/v) NaN$_3$ and 7% D$_2$O for NMR studies.

NMR—NMR samples for Rub1 monomer were prepared in 20 mM phosphate buffer (pH 6.0), which was used for structural characterization. All NMR binding studies were done in 20 mM phosphate buffer (pH 6.8). NMR data were acquired at 22.5 °C on a Bruker Avance III 600 MHz spectrometer equipped with a cryoprobe. Details of the experiments performed and data analysis can be found in the supplemental information.

Mammalian Cell Culture, Transfection, and Ni-affinity Purification—H1299 cells were cultured in Dulbecco's modified Eagle's medium with 10% (v/v) fetal bovine serum. Cells at 90% confluency in 6 cm plates were transfected using Lipofectamine 2000 as described elsewhere (43). Twenty to twenty-four hours after transfection, the cells were lysed in 500 μl Gd-HCl buffer (6 M guanidinium HCl, 100 mM phosphate buffer pH 8.0, 10 mM imidazol, 10 mM β-mercaptoethanol, 1 mM pefabloc, 1 μg/ml apeptin/leupeptin mixture), and 20 μl of protein A Sepharose beads (equilibrated in Gd-HCl buffer) were added. The samples were incubated at 4 °C with rotation for 1 h and then centrifuged, and 50 μl of Ni-agarose beads (equilibrated in Gd-HCl buffer) were added to the supernatant; this was followed by incubation at 4 °C for 3 to 4 h or overnight. The beads were then washed two times with Gd-HCl buffer, and this was followed by two more washes in a buffer containing one part Gd-HCl buffer and four parts 50 mM Tris-Cl (pH 6.8) containing 20 mM imidazol. Finally, the samples were washed two times with 50 mM Tris-Cl (pH 6.8) buffer containing 20 mM imidazol. The samples were boiled at 95 °C for 5 min in 100 μl of Laemmli buffer containing 200 mM imidazole and loaded onto SDS-PAGE gels.

Cleavage of Rub1-Ub Dimer—0.1 mM of K48-linked Rub1-Ub 74 dimer was incubated with either 26S proteasome or COP9 signalosome or with both in the presence of 100 mM Tris-Cl buffer (pH 7.4), 20% glycerol, 20 mM MgCl$_2$, 0.5 M phosphocreatine, 0.2 mg/ml phosphocreatinine kinase, 0.5 M ATP, and 1 M DTT. The reaction was incubated for 12 to 16 h at 30 °C.

Stable Isotope Labeling of Amino Acids in Cell Culture and Data Analysis—RGS-His$_6$-Rub1-expressing yeast cells were grown in minimal synthetic defined (SD) media containing yeast nitrogen base and glucose supplemented with 4 mg/l ^{13}C$_6$^{15}N$_2$ lysine and 2 mg/l ^{13}C$_6$^{15}N$_4$ arginine (Cambridge Isotope Laboratories Inc, Andover, MA, USA.), and RGS-His$_6$-empty vector expressing cells in SD media supplemented with 4 mg/l ^{12}C$_6$^{14}N$_2$ lysine and 2 mg/l ^{12}C$_6$^{14}N$_4$ arginine (Sigma Aldrich). Cells were lysed and enriched for Rub1 via the use of a mini nickel-nitrilotriacetic acid column (Qiagen, Valencia, CA, USA). Eluted proteins were separated via SDS-PAGE and cut into 12 gel slices. The gel slices were incubated with modified trypsin (Promega, Madison, WI, USA), and the resulting tryptic peptides were identified by means of mass spectrometry. Details of the in-gel tryptic digestion and mass spectrometric analysis are included in the supplemental information.
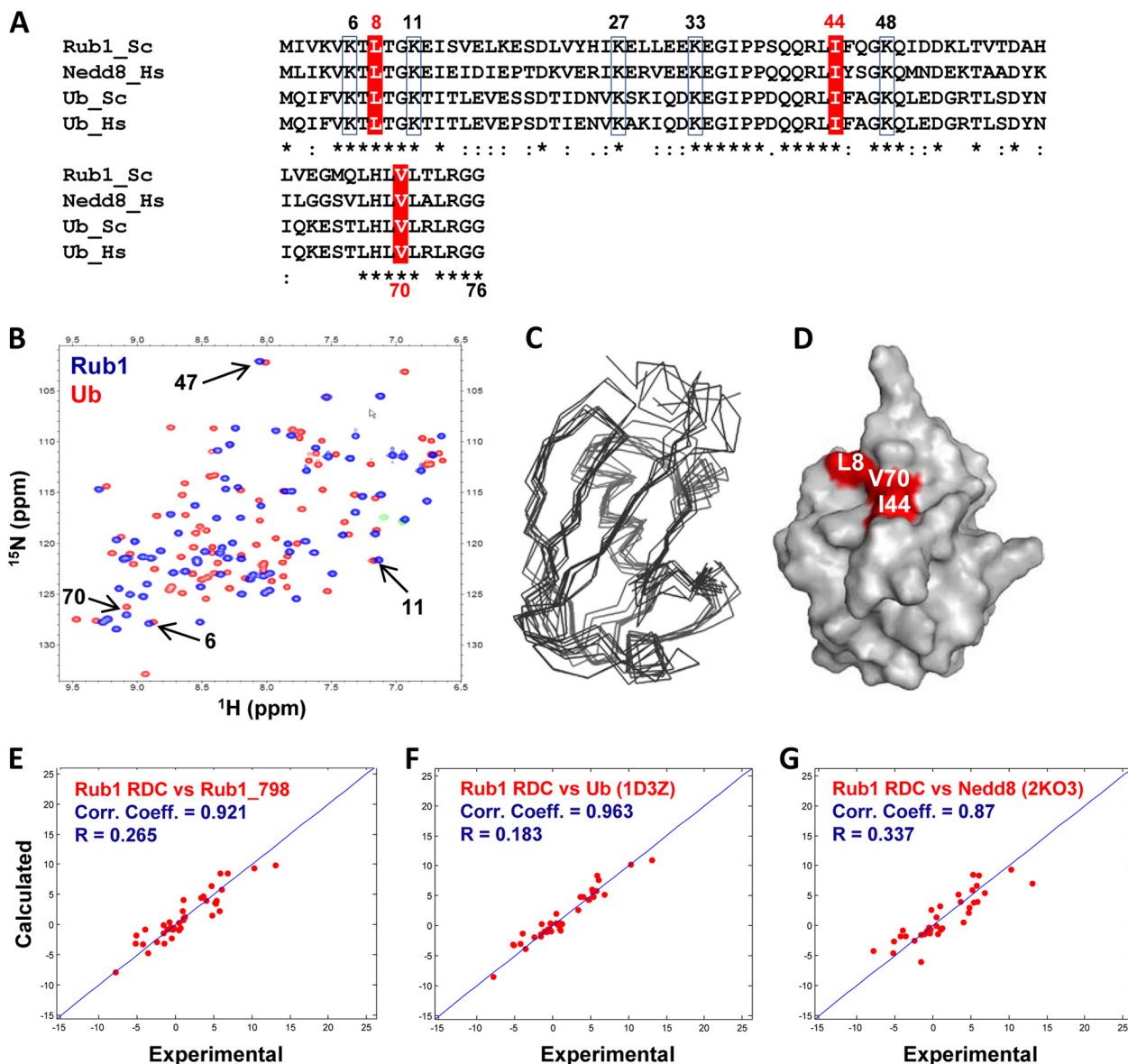
FIG. 1. **Rub1 is structurally similar to Ub.** *A*, amino acid sequence comparison of Ub and Rub1/Nedd8 from *Saccharomyces cerevisiae* (Sc) and human (Hs). Lysine residues that are conserved in both Ub and Rub1 are represented by empty boxes. The hydrophobic patch residues (L8, I44, and V70) are shaded red. Shown here are sequences of mature proteins; the sequences of the non-processed proteins contain an additional C-terminal N for Rub1 and residues GGLGQ for Nedd8. *B*, ^{1}H-^{15}N HSQC spectrum of Rub1 (blue) overlaid with the similar spectrum of Ub (red). Selected residues that have similar chemical shifts in both Rub1 and Ub are marked with numbers and indicated by arrows. *C*, an ensemble of the nine lowest energy structures of Rub1 (backbone trace) generated by CS-Rosetta. *D*, surface representation of one of the CS-Rosetta-generated structures of Rub1 (Rub1_798). The conserved hydrophobic patch residues are painted red and are indicated. *E–G*, the agreement between experimentally measured residual dipolar couplings (RDCs) of Rub1 and the back-calculated RDCs using the structures of Rub1_798 (*E*), Ub (*F*; PDB ID: 1D3Z), or Nedd8 (*G*; PDB ID: 2KO3). The diagonal represents absolute agreement. Pearson's correlation coefficient (Corr. Coeff.) and the quality factor (R) are indicated.

Pulldowns of Ub Receptors with Rub1—Purified recombinant His$_6$-Rub1 or His$_6$-Ub, immobilized on CH Sepharose 4B beads, were incubated with whole cell extract prepared from natively lysed Δ*rub1* cells. 2 ml of cell extract were incubated with 150 μl slurry (Rub1 or Ub conjugated, or mock) overnight at 4 °C. The beads were washed with 20 column volumes of lysis/wash buffer, followed by elutions with 1 M NaCl or 8 M urea. Hydrophilic and hydrophobic eluates were separated via SDS-PAGE and immunoblotted against Rpn10 and Dsk2.

RESULTS

Rub1 Is Structurally Similar to Ubiquitin—Although Rub1 is an important protein in *Sachharomyces cerevisiae*, its three-dimensional structure was not known. NMR spectra of Rub1 indicate a well-folded protein and show striking similarity to analogous spectra of Ub (Fig. 1*B*). To determine the structure of Rub1, we obtained a nearly complete NMR resonance

assignment of ^{1}H, ^{13}C (C', Cα, Cβ), and amide ^{15}N nuclei of this protein. Using these resonances along with predictions of protein backbone dihedral angles made by TALOS+ (44), we computed a model structure of Rub1 using the CS-Rosetta approach (45, 46), which resulted in an ensemble of nine closely related low-energy structures (Fig. 1C). To verify these predicted structures, we measured residual dipolar couplings (RDCs) for backbone amide groups of Rub1 in a weakly aligned liquid-crystalline medium. Comparison of these RDC data with the predictions based on CS-Rosetta-generated structures showed good general agreement for all structures, with the Pearson's correlation coefficient values ranging from 0.743 to 0.921 (supplemental Table S3). This suggests that (i) these structural models provide a good representation of the Rub1 structure and (ii) our NMR signal assignments can be used to map Rub1's interactions with other proteins. The structure that gave the best agreement (shown in Figs. 1D and 1E) is used throughout this paper as the representative structure of Rub1. Furthermore, the RDC data for Rub1 are also in good agreement with the published structures of Ub and Nedd8 (Figs. 1F and 1G), directly indicating that Rub1 is structurally very similar to Ub and Nedd8. Indeed, the predicted model structure of Rub1 can be superimposed on the published structures of Ub and Nedd8 with backbone (Cα) root-mean-square deviations of 0.998 Å and 1.185 Å, respectively (supplemental Fig. S1A). The distribution of surface charges on the β-sheet side of Rub1 encompassing the hydrophobic-patch residues L8, I44, and V70 (functionally important in Ub) is very similar to that of Ub and Nedd8 (supplemental Fig. S1B), suggesting similar ligand binding properties.

Rub1 Binds to Non-proteasomal Ub Receptors/Shuttles— There are three well-studied non-proteasomal Ub receptors/shuttles: Rad23 (its human orthologue is known as hHR23a) (47, 48), Dsk2 (known as hPLIC1 or Ubiquilin 1 (UQ1) in humans) (49), and Ddi1[1] (50, 51). All of them are unique in that they contain an N-terminal Ub-like (UBL) domain that binds to the proteasome via Rpn1 (42, 52, 53) and a C-terminal Ub-associated (UBA) domain that binds to Ub chains (54, 55). These UBL-UBA proteins have been seen to cycle on and off the proteasome while delivering the ubiquitinated cargo from the cytoplasm and the nucleus to the proteasome, which is why they are also known as shuttle proteins (56, 57). Although

a Ub chain is the preferred binding partner of these shuttle proteins, monoubiquitin (monoUb) has been shown to interact with them as well, albeit with lower affinity (58–62). Moreover, as Rub1 is documented to form monomeric modifications on its targets (26, 28), comparison of its binding preferences with monoUb might unlock a clue as to what distinguishes the two. To assess whether Rub1 interacts with the UBA domains of these receptors, ^{15}N labeled Rub1 was titrated with the UBA domains of hHR23a, human UQ1, and yeast Ddi1, and the interaction was monitored using NMR spectroscopy (see Fig. 2 and below for further details).

NMR signals are highly sensitive to the local electronic environment in a molecule (63, 64) and therefore have been widely used to map the interacting surfaces (13, 14, 58, 65, 66) and assess the strength of binding (14, 58, 59, 66–68). A perturbation in the local environment in a protein could result in a shift of the NMR signal from its original position (referred to as chemical shift perturbation (CSP)) or broadening (attenuation) of the NMR signal, or both. As both CSPs and signal attenuations are direct consequences of a change in the local environment in a protein caused by complex formation, they can be used as markers to map the binding interface.

Rub1 Interaction with the UBA2 Domain of hHR23a— Rad23 contains two UBA domains: a central UBA1 domain and a C-terminal UBA2 domain. Both UBA domains interact with monoUb and have a binding preference for K48-linked chains (61, 69, 70). To test whether the UBA2 domain interacts with Rub1, unlabeled UBA2 domain of the human orthologue of Rad23 (hHR23a) was added to ^{15}N labeled Rub1. Analysis of the NMR spectra revealed site-specific CSPs for many Rub1 residues, indicating a Rub1–UBA2 interaction (Fig. 2A). The observed CSPs increased with increasing amounts of UBA2 and almost saturated at UBA2:Rub1 molar ratios in the range of 3:1 to 4:1 (Fig. 2C). Additionally, many amides showed signal attenuations indicative of intermediate or slow exchange on the NMR chemical shift time scale (Fig. 2A). Mapping the perturbations onto the surface of Rub1 revealed that they were clustered on one side of the molecule and included the hydrophobic patch residues L8, I44, and V70 (Fig. 2B), in striking similarity to the UBA2-interacting surface of monoUb (71).

To assess the stoichiometry of the UBA2:Rub1 complex, we measured the longitudinal ^{15}N relaxation time (T_1), which is a sensitive indicator of the overall tumbling rate of the molecule/complex and therefore is directly related to its apparent size. The average T_1 value measured for the UBA2:Rub1 complex at a 4:1 molar ratio was 634 $\pm$ 31 ms (see Table I), which corresponds to a molecular weight of 14 to 15 kDa (58). This result is consistent with a 1:1 stoichiometry of the UBA2/Rub1 complex (the expected molecular mass = 14 kDa). We then assessed the affinity of the interaction by fitting our titration data to a one-site binding model, which yielded a K_d value of 72 $\pm$ 17 μM, averaged over six residues (Table II, and

---

[1] The abbreviations used are: Ddi1, DNA damage inducible protein 1; E1, ubiquitin-activating enzyme; E2, ubiquitin-conjugating enzyme; E3, isopeptide ligase enzyme; HA, hemagglutinin; hHR23a, human homologue of Rad23 protein A; Nedd8, neuronal precursor cell expressed developmentally down-regulated protein 8; NMR, nuclear magnetic resonance; NUB1, NEDD8 ultimate buster 1; NUB1L, NEDD8 ultimate buster 1-long; PDB, Protein Data Bank; Rub1, related to ubiquitin protein 1; SILAC, stable isotope labeling of amino acids in cell culture; Ub, ubiquitin; UBA, ubiquitin-associated protein; UBL, ubiquitin-like protein; UIM, ubiquitin-interacting motif; UQ1, ubiquilin 1.
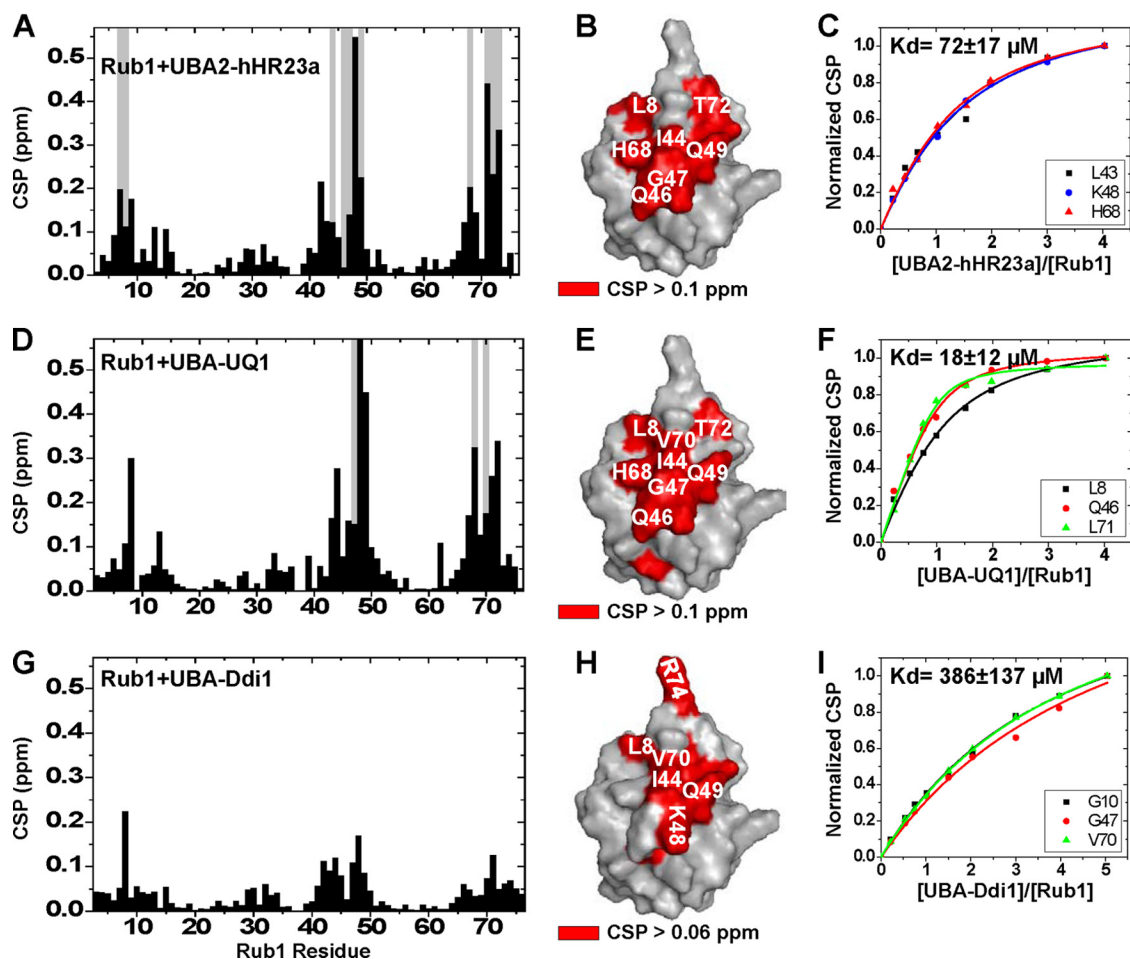
FIG. 2. **Interaction of Rub1 with the UBA domains of the shuttle proteins.** Chemical shift perturbations (CSPs) (black bars) and significant signal attenuations (>75%; gray bars) in Rub1, plotted as a function of the residue number, at the end point of titration with UBA2-hHR23a (*A*), UBA-UQ1 (*D*), or UBA-Ddi1 (*G*). Mapping of the Rub1 residues (red) exhibiting CSPs higher than indicated and/or significant signal attenuations upon binding to UBA2-hHR23a (*B*), UBA-UQ1 (*E*), or UBA-Ddi1 (*H*). Representative titration curves showing the normalized CSPs (in Rub1) as a function of ligand/protein molar ratio for UBA2-hHR23a (*C*), UBA-UQ1 (*F*), or UBA-Ddi1 (*I*) interactions with Rub1. The lines represent the results of fitting.

TABLE I

Longitudinal ^{15}N relaxation time (T_1, in ms) for the unbound proteins or the protein/ligand complexes at the endpoint of the titration

Protein	Unbound	+UBA-UQ1	+UBA2-hHR23a	+UBA-Ddi1	+UIM-Rpn10
MonoRub1	459 ± 33	647 ± 44	634 ± 31	543 ± 27	499 ± 33
Proximal-Ub, heterodimer	694 ± 42	1000 ± 62	1054 ± 85	874 ± 56	1103 ± 192
Distal-Rub1, heterodimer	680 ± 45	974 ± 67	1040 ± 88	829 ± 57	968 ± 90

The T_1 data reported here represent the mean and the standard deviation calculated over several backbone amide signals.

also see Fig. 2*C*). This affinity is ~4- to 5-fold higher than the reported affinity of UBA2 for monoUb (400 ± 100 μM (71, 72)).

Rub1 Interaction with the UBA Domain of UQ1—Unlike hHR23a, human UQ1 (also known as hPLIC1) contains only one UBA domain, located at the C terminus (73), and has been shown to be the strongest Ub binder among the family of UBL-UBA proteins (61, 74). We detected a relatively strong interaction between Rub1 and the UBA2 domain of hHR23a, and we were interested to know whether Rub1 binds also to the UBA domain of UQ1 (UBA-UQ1). Indeed, our NMR data

confirmed this interaction. Moreover, NMR signal perturbations (CSPs and signal attenuations) in Rub1 caused by UBA-UQ1 binding indicate that this interaction is highly specific and involves predominantly residues clustered around the hydrophobic patch on Rub1's surface (Figs. 2*D* and 2*E*). The UBA-UQ1-interaction surface on Rub1 is similar to that on Ub (59), as well as to the Rub1 surface involved in hHR23a UBA2 binding (Figs. 2*A* and 2*B*). A ^{15}N T_1 of 647 ± 44 ms for the Rub1/UBA-UQ1 complex suggests a 1:1 binding (Table I). The quantitative analysis of the CSPs of Rub1 upon titration with

Protein	UBA-UQ1 (μM)	UBA2-hHR23a (μM)	UBA-Ddi1 (μM)	UIM-Rpn10
monoRub1	18 ± 12	72 ± 17	386 ± 137	? (mM)
Proximal-Ub, heterodimer	6 ± 7	52 ± 27	130 ± 45	36 ± 9 μM
Distal-Rub1, heterodimer	50 ± 20	50 ± 22	150 ± 37	185 ± 103 μM

The dissociation constants reported here represent the mean and the standard deviation calculated over at least four residues (see supplemental Table S4).
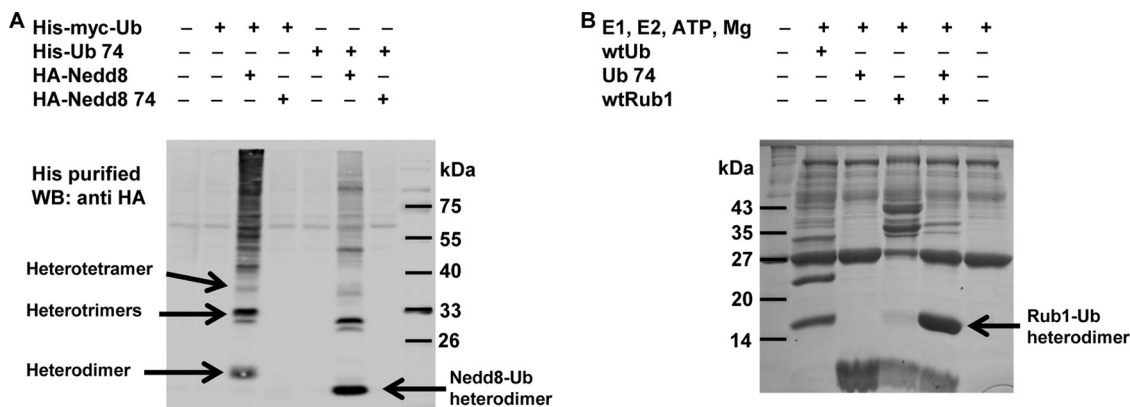

FIG. 3. **Formation of the Rub1-Ub heterodimer both within cells and *in vitro*.** *A*, 1 μg of each plasmid expressing His-myc-Ub or its mutant (His-Ub 74) and HA-Nedd8 or its mutant (HA-Nedd8 74) were transfected into H1299 cells, as indicated. (In all these constructs, the tags were N-terminal and thus did not interfere with conjugation.) After 20 to 24 h of transfection, cells were lysed in denaturing guanidinium hydrochloride buffer. His-Ub conjugated proteins were purified by Ni-beads followed by SDS-PAGE and Western blotting with an HA antibody. The running positions of the heterodimer, heterotrimer, and heterotetramer are shown by arrows. *B*, 100 μM of purified recombinant proteins (Ub, Ub 74, Rub1), as indicated, were incubated with 300 nM of Ub E1 and 20 μM of E2–25K in a ubiquitination reaction. The reaction was incubated at 30 °C overnight (12 to 16 h). The reaction mixture was separated on SDS-PAGE, and this was followed by staining with Coomassie blue. The running position of the Rub1-Ub 74 heterodimer is indicated by the arrow.

UBA-UQ1 yielded a K_d of 18 ± 12 μM (Fig. 2*F* and Table II), indicating that the monomeric Rub1 has a stronger affinity for UBA-UQ1 than for the UBA2 domain of hHR23a. Note that this affinity is essentially the same as that observed for UBA-UQ1 interaction with Ub (59). Interestingly, six residues in Rub1 exhibited slow-exchange behavior in which an appearance of a second signal corresponding to the bound state was observed. Taking advantage of this, we independently determined the K_d from the ratio of the signals corresponding to the free and bound states in slow exchange. Assuming 1:1 binding at [UBA-UQ1]:[Rub1] ≤ 1, we obtained a K_d value of 21 ± 14 μM, averaged over five residues, which is in excellent agreement with that derived from fitting the titration curves. All these data indicate that isolated Rub1 interacts with UBA-UQ1 essentially as Ub does, that is, through the same (hydrophobic patch) surface and with comparable affinity.

Rub1 Interaction with the UBA Domain of Ddi1—Prior data have established that Ddi1 is the weakest Ub binder among the UBL-UBA proteins (60, 69). The budding yeast Ddi1 protein contains a C-terminal UBA domain that has been shown to bind Ub (60). Our NMR titration data show that Rub1 also interacts with the UBA domain of yeast Ddi1 and through the same hydrophobic patch as with the UBA domains of hHR23a and UQ1 (Figs. 2*G* and 2*H*). The titration curves for many residues fit best the 1:1 binding model, yielding a K_d value of

386 ± 137 μM (averaged over eight residues; Table II and Fig. 2*I*), suggesting a weak interaction.

A Rub1-Ub Heterodimer Can Be Synthesized Both within Cells and in Vitro—Given the interaction observed for Rub1 with the Ub chain-binding domains of all three non-proteasomal receptors/shuttles, and knowing that some substrates may be modified by Rub1, Ub, or both, we next aimed to evaluate whether Rub1 forms a chain within cells. Examples of both contradictory and concordant evidence lead to debate about the chain-forming ability of Rub1 (75–78). Ub has seven lysine residues (K6, K11, K27, K29, K33, K48, and K63), and all of them have been shown to be involved in chain formation *in vivo* (79–81). However, despite having five of those lysine residues (K6, K11, K27, K33, and K48) conserved from yeast to human (Fig. 1*A*), Rub1/Nedd8 has not been directly shown to efficiently form a polymer within cells. To address this question, and in order to distinguish between Rub1/Nedd8 and Ub, we transfected a human lung cancerous cell line (H1299) with plasmids expressing His-tagged Ub (His-Ub) and HA-tagged Nedd8 (HA-Nedd8). Twenty to twenty-four hours post-transfection, cells were lysed in 6 M guanidinium hydrochloride buffer followed by Ni-bead purification. Proteins were separated via SDS-PAGE and blotted with an HA-antibody. Interestingly, we observed many proteins modified with both Ub and Nedd8 in these cells (Fig. 3*A*, lane 3).

The appearance of high molecular weight smear (>55 kDa) indicates targets that are simultaneously modified with both Ub and Nedd8. They may be in mixed chain or "in trans" on different sites on the target, or both. Moreover, a protein running at around 20 kDa was also observed. Because this protein must contain at least one molecule of His-Ub and one molecule of HA-Nedd8, we conclude that this is a substrate-free Nedd8-Ub heterodimer. Similarly, two bands running at around 30 kDa were also observed, and most probably they are Nedd8-Ub heterotrimers in which, in contrast to the heterodimer, the slower running band may have an extra molecule of either His-Ub or HA-Nedd8 attached while the faster running band likely contains an extra (untagged) endogenous Ub or Nedd8. Similarly, a presumable heterotetramer was also observed running somewhat below 40 kDa. Altogether our data show that a Nedd8-Ub chain exists within cells. To separately validate this, we also showed that this type of chain exists within *Sachharomyces cerevisiae* by utilizing stable isotopic labeling of amino acids in cell culture (SILAC) and mass spectrometric analysis (see supplemental Fig. S2).

The observation of Nedd8-Ub heterologous chains intrigued us and motivated us to determine the order of the linkages in these chains (*i.e.* whether Nedd8 is ubiquitinated or Ub is neddylated). To this end, we transfected H1299 with a plasmid expressing His-Ub along with another plasmid expressing a mutant of HA-Nedd8 in which two glycines at the carboxyl terminus of Nedd8 were deleted (HA-Nedd8 74). By doing this, we ensured that HA-Nedd8 74 could not be activated by E1 and thus could not be attached to any substrate, including Ub; however, this truncated Nedd8 variant could still be used as a substrate to take Ub onto any of its lysine residues. Notably, we did not observe the presence of the Nedd8-Ub heterodimer, which indicates that the lysine residues of Nedd8 could not be used to form these heterodimers (Fig. 3*A*, lane 4). This further suggests that Ub's lysine residue(s) has been used to synthesize these substrate-free Nedd8-Ub dimers. If this is the case, we should expect the Nedd8-Ub dimer to reappear upon transfection of the cells with a plasmid expressing HA-Nedd8 along with another plasmid expressing His-Ub 74 (in which two glycines were deleted at the C terminus of Ub). Indeed, the Nedd8-Ub heterodimer reappeared (Fig. 3*A*, lane 6), indicating that Ub is neddylated. These results clearly demonstrate that Nedd8 acts as a Ub chain terminator. Consistent with this notion, our SILAC experiment in yeast cells identified K48 linkage only on Ub and not on Rub1 (supplemental Fig. S2), which supports our theory that Rub1 can serve to cap Ub tags.

In order to further study the structural and functional properties of the Nedd8-Ub heterologous chain, we set up *in vitro* reactions with either E1 of Ub or E1 of Nedd8 along with well-known Ubs E2s, E2–25K, or Ubc13/Mms2, shown to synthesize unanchored Ub chains selectively linked via K48 (82, 83) or K63 (84, 85), respectively. Surprisingly, with E1 of Ub but not with E1 of Nedd8, either E2–25K or Ubc13/Mms2

was able to efficiently synthesize heterologous dimers containing Ub 74 and wtRub1 (Fig. 3*B* and supplemental Fig. S3). However, wtRub1 alone did not form any free chain efficiently; instead it modified the E2–25K (bands appeared in and migrated slower than E2–25K running position in Fig. 3*B*, lane 4). This suggests that Rub1 is indeed efficiently utilized by the Ub system under the condition used, and it is either conjugated to the available Ub or, in the absence of Ub, transferred to a lysine of E2–25K. Furthermore, mass spectrometric analysis confirmed that these dimers indeed consist of Rub1 linked via its C-terminal glycine to K48 of Ub (supplemental Fig. S4). This is similar to what we observed in H1299 cells, in which lysine residues of Nedd8 cannot be used to form these heterologous dimers. However, the C terminus of Nedd8 can be attached to a lysine residue of Ub; therefore, we conclude that Nedd8 acts as a chain terminator. Mutational analysis of Ub (K48R and K63R) further showed that these dimers were linked via K48 when E2–25K was used or via K63 when Ubc13/Mms2 was used (supplemental Fig. S3*B*), which also indicates that these E2s preserve their properties to form specific linkages. This also suggests that, like Ub, Rub1/Nedd8 can be incorporated into differently linked chains (*i.e.* attached to different lysines on Ub) depending on the E2 enzyme responsible for the conjugation. We obtained similar results using either Rub1 or Nedd8, and thus for further study we used Rub1-Ub dimer for structural and functional characterization.

K48-linked Rub1-Ub Heterodimer Forms an Interface Similar to That in K48-linked Ub Homodimer—We and others have previously shown that a K48-linked Ub dimer at near-neutral pH adopts a "closed" conformation in which the interface is formed by the hydrophobic patches (consisting of L8, I44, and V70) of the two Ubs (12, 13). To determine whether a K48-linked Rub1-Ub heterodimer adopts a similar conformation, we recorded a ^{1}H-^{15}N NMR spectrum at near-neutral pH (6.8) of the heterodimer in which both Rub1 and Ub were labeled with ^{15}N (Figs. 4*A* and 4*B*). The NMR signals from both proteins were well spread and did not overlap with each other (except for T9). The CSP plots for the heterodimer show perturbations at the C terminus of Rub1 and near K48 of Ub, which are expected because of the formation of the G76-K48 isopeptide bond (Fig. 4*C*). In addition, significant and site-specific perturbations were also observed for residues 7, 36, 42, 68, and 70 of Rub1 and 7, 13, 45, 59, 68, and 70 of Ub. These perturbations are likely due to noncovalent interactions between Rub1 and Ub in the heterodimer. Mapping the interdomain interaction surfaces onto the structure of Rub1 and Ub shows that most of the perturbations are located on one side of the respective molecule that includes the hydrophobic patch (Figs. 4*D* and 4*E*). These interactions are very similar to those observed in K48-linked diubiquitin (diUb) (13), and when mapped on a putative Rub1-Ub structure modeled by analogy with the closed structure of K48-linked Ub homodimer (Figs. 4*F*–4*H*), they are all located at the
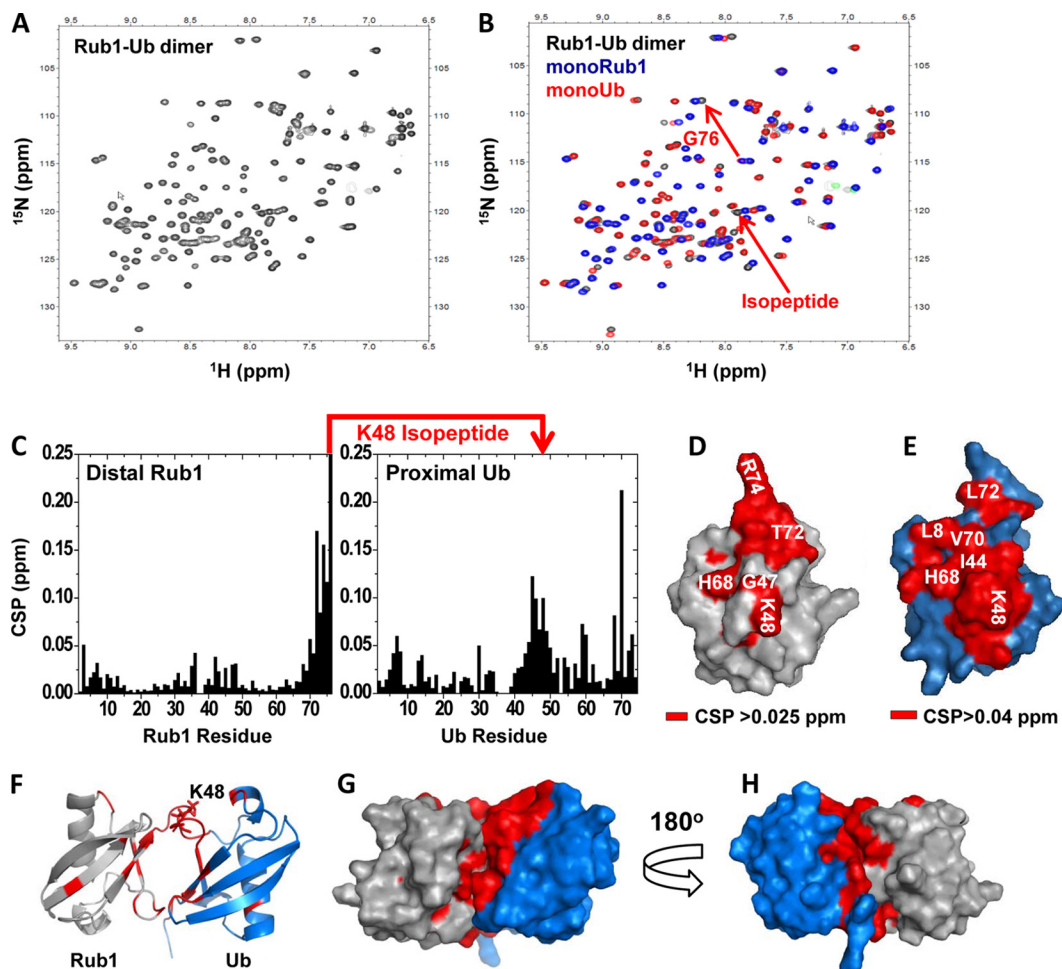
FIG. 4. **K48-linked Rub1-Ub heterodimer forms an interface similar to the interface formed by Ub-Ub homodimer.** *A*, ^{1}H-^{15}N HSQC spectrum (at neutral pH) of the Rub1-Ub heterodimer in which both distal (Rub1) and proximal (Ub) units were ^{15}N labeled simultaneously. *B*, overlay of the spectrum of the Rub1-Ub heterodimer (black) with the spectra of monomeric Rub1 (blue) and Ub (red). The signal shift of G76 in Rub1 and the appearance of a signal from the isopeptide N–H group (ε-N of K48 in Ub), both caused by the isopeptide bond formation, are indicated with arrows. *C*, the backbone amide CSPs of Rub1 and Ub, due to the formation of the heterodimer, were plotted as a function of their residue numbers. The residues of Rub1 (G76) and Ub (K48) involved in linkage formation are indicated by a connecting arrow. *D, E,* mapping (marked in red) of the perturbed residues (CSPs > 0.025 ppm in the case of Rub1 and > 0.04 ppm in the case of Ub) on the surface of Rub1 (*D*) and Ub (*E*). *F–H,* the perturbed residues in Rub1 and Ub (colored red, from panels *D* and *E*) are mapped on the putative structure model of the Rub1-Ub heterodimer (shown as a ribbon (*F*) and as a surface representation (*G, H*)). This model was obtained from the structure of K48-linked diUb (PDB ID: 1AAR) by superimposing Rub1 onto the distal Ub.

interdomain interface and in the linker region. Also, the [15]N T_1 values (Table I) are essentially the same for both domains (suggesting that they tumble together as a one unit) and almost identical to those observed for K48-linked diUb (58). All these results indicate that the Rub1-Ub heterodimer forms an interface similar to that in the Ub-Ub homodimer.

Rub1-Ub Heterodimer Interacts with the Shuttle Proteins of the Ub Pathway—The role of K48-linked Ub chains in targeting substrates for proteasomal degradation has been well documented (86, 87). To successfully degrade the substrates, these chains are required to be recognized by the proteasomal receptors and/or the UBL-UBA shuttle proteins (6, 88, 89). Although tetraUb is an efficient signal for proteasomal degradation, we previously showed that K48-linked diUb is

the structural building block in tetraUb (12, 13, 90), and therefore diUb has been used to functionally characterize the interaction of the K48-linked chains with their receptors. To examine whether and how the heterodimer is recognized by the shuttle proteins, a ^{15}N-labeled K48-linked Rub1-Ub construct was titrated with the UBA domains of hHR23a, UQ1, and Ddi1, and the binding was monitored using NMR spectroscopy. Interestingly, the Rub1-Ub heterodimer bound to the UBA domains of all three shuttle proteins tested (see Fig. 5 and below for further details).

To map the interface on the Rub1-Ub heterodimer involved in binding to the UBA2-hHR23a domain, we analyzed the CSPs along with signal attenuations. This revealed that the distal Rub1 subunit interacts with the UBA2 domain through
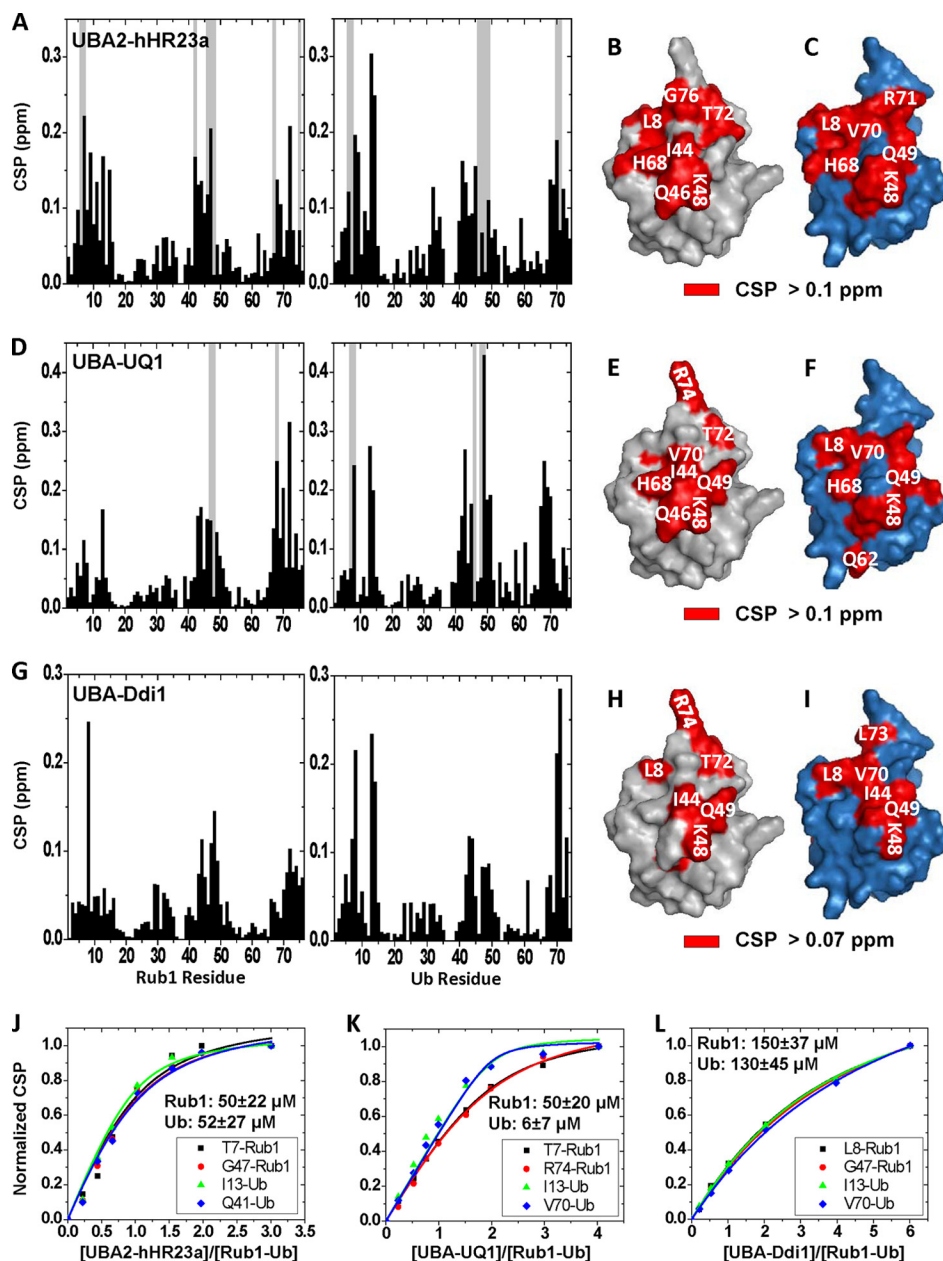
FIG. 5. **The Rub1-Ub heterodimer interacts with the UBA domains of the shuttle proteins.** The backbone amide CSPs (black bars) and significant signal attenuations (>75%, shown by gray bars) in the Rub1-Ub heterodimer at the end point of titration with the UBA2-hHR23a (A), UBA-UQ1 (D), or UBA-Ddi1 (G), plotted as a function of the residue number. Surface map of the residues perturbed in the distal Rub1 (left, gray) and proximal Ub (right, blue) of the heterodimer upon the addition of a saturating amount of UBA2-hHR23a (B, C), UBA-UQ1 (E, F), or UBA-Ddi1 (H, I). Shown in red are residues showing significant CSPs, as indicated, and/or strong signal attenuations. The representative titration curves are shown for each titration: Rub1-Ub/UBA2-hHR23a (J), Rub1-Ub/UBA-UQ1 (K), or Rub1-Ub/UBA-Ddi1 (L).

essentially the same surface as in monoRub1-UBA2 interaction (Figs. 5A–5C). Moreover, the proximal Ub interaction with the UBA2 domain was essentially the same as reported previously for the proximal Ub of the K48-linked diUb (58). To analyze the stoichiometry of the UBA2:Rub1-Ub complex, we measured T_1 at the end point of titration (3:1 molar ratio). The average T_1 value measured for the UBA2:Rub1-Ub complex was 1047 ± 87 ms (Table I). This corresponds to a molecular

weight of 26 to 31 kDa, consistent with two UBA2 molecules bound to one molecule of the heterodimer. However, the titration curves for many residues in the heterodimer fit well to a model that assumes that only one UBA2 molecule binds to one molecule of the heterodimer (1:1 interaction). This is plausible when one UBA2 molecule binds at the beginning of titration when the concentration of the UBA2 is lower than the heterodimer concentration ([UBA2]:[heterodimer] <1.0). How-

ever, at the later points in titration, when the UBA2 is present in excess relative to the heterodimer ([UBA2]:[heterodimer] >1.0), a second UBA2 molecule binds, shifting the stoichiometry from 1:1 to 2:1. This mode of binding is very similar to that observed in sandwich-like complex formation between UBA2 and a K48-linked diUb (58). Indeed, a careful analysis of the directions of NMR signal shifts (in the ^{1}H-^{15}N coordinates/spectra) during the titrations of monoRub1 and the distal Rub1 with UBA2 suggests differences in the local interface contacts involved in these two interactions (supplemental Fig. S5A). Further analysis of the titration data yielded K_d values of 50 $\pm$ 22 μM for the distal Rub1 and 52 $\pm$ 27 μM for the proximal Ub (averaged over seven and nine residues, respectively; see Table II and Fig. 5J), which suggests that the UBA2 binds to both subunits with similar affinity.

We next mapped the interacting surface on both Rub1 and Ub units in the K48-linked heterodimer upon the addition of unlabeled UBA-UQ1. A careful analysis of the mapped surfaces indicates that the Rub1 unit in the heterodimer binds UBA-UQ1 the same way that monoRub1 does (Figs. 5D–5F). Indeed, the directions of signal shifts (in the ^{1}H-^{15}N coordinates) in the monoRub1:UBA-UQ1 and the distal Rub1:UBA-UQ1 titrations are very similar to each other. This confirms that the distal Rub1 in the heterodimer binds UBA-UQ1 essentially involving the same surface as in the case of monoRub1:UBA-UQ1 interaction (supplemental Fig. S5B). Furthermore, the UBA-interacting surface of Ub in the heterodimer is very similar to that in monoUb:UBA-UQ1 interaction (59). This suggests that both subunits in the heterodimer bind one molecule of UBA-UQ1 each. Indeed, our ^{15}N T_1 relaxation measurements for the UBA-UQ1:Rub1-Ub complex yielded a value of 987 $\pm$ 65 ms (Table I), which corresponds to a molecular mass of 25 to 28 kDa, consistent with a 2:1 stoichiometry of the UBA-UQ1:Rub1-Ub complex. Further analysis of the titration data yielded a K_d of 50 $\pm$ 20 μM for the distal Rub1 and of 6 $\pm$ 7 μM for proximal Ub, which suggests that UBA-UQ1 binds to Ub in the heterodimer tighter than to the distal Rub1. This binding mode is similar to that observed for the Ub homodimer, in which the two Ub units bind UBA-UQ1 independently of each other (59).

The Rub1 subunit in the heterodimer also binds the UBA domain of Ddi1, and through the same surface as in the case of monoRub1 (Figs. 5G–5I). The titration curves for both distal Rub1 and proximal Ub residues fit best to a binding model assuming 2:1 stoichiometry (UBA:heterodimer), suggesting, like in UBA-UQ1 binding, that both domains in the Rub1-Ub heterodimer each interact with one molecule of UBA-Ddi1. The calculated K_d was 150 $\pm$ 37 μM for the distal Rub1 and 130 $\pm$ 45 μM for the proximal Ub (averaged over 10 and 9 residues, respectively). This indicates that the interaction of the UBA domain of Ddi1 with the Rub1-Ub heterodimer is the weakest among the three UBL-UBA proteins tested, consistent with the notion that the UBA domain of Ddi1 binds Ub and polyUb chains weakly.

Rub1-Ub Heterodimer Is Recognized by the Proteasome and Processed by Both the Proteasome and the Signalosome—Yeast proteasome contains two intrinsic Ub receptors, Rpn10 and Rpn13, and both of them have been shown to contain a well-defined Ub binding domain (91, 92). Rpn10 binds Ub through its highly conserved Ub interacting motif (UIM), whereas Rpn13 has been shown to interact with Ub via a pleckstrin motif. In addition to these two intrinsic receptors, a third subunit in mammalian proteasome, Rpt5 (93), has been shown to cross-link to Ub chains via a mechanism that remains to be determined. Among these receptors, the UIM domain of Rpn10 has been most studied and is believed to bind Ub chains directly (56). Moreover, the UIM domain of another protein, UBXD7, has been shown to bind to conjugated Nedd8 on CUL2 (94, 95). This inspired us to examine whether Rub1 and the Rub1-Ub heterodimer interact with the UIM domain of Rpn10. For this, we titrated either ^{15}N-labeled Rub1 or the ^{15}N-labeled Rub1-Ub heterodimer with unlabeled UIM of yeast Rpn10. The observed CSPs for monoRub1 were very weak (the maximal CSP observed was 0.065 ppm for K48) at a 3:1 ratio of [UIM]:[Rub1] (Fig 6A). The perturbed residues cluster in and around the hydrophobic patch of Rub1 (Fig. 6D), similar to Ub–Rpn10 interaction (66), suggesting that Rub1 does bind the UIM domain of Rpn10, albeit weakly. Furthermore, the analysis of the titration curves did not yield a consistent K_d because of the small CSPs observed. To confirm that Rub1 binds the UIM weakly, we measured the ^{15}N T_1 of monomeric Rub1 and of the UIM:Rub1 complex (3:1 ratio) separately. The average T_1 values for Rub1 and the UIM:Rub1 complex were 459 $\pm$ 33 ms and 499 $\pm$ 33 ms, respectively. A detailed analysis revealed a systematic increase in T_1 values for many Rub1 residues upon addition of the UIM domain of Rpn10. However, the average T_1 was not near the value of ca. 700 ms expected for the UIM:Rub1 complex (18 kDa), suggesting that only a small fraction of Rub1 is in the UIM-bound state at these conditions. This confirms that although Rub1 does interact with the UIM domain of Rpn10, the affinity is very weak.

Analysis of the titration data for ^{15}N-labeled Rub1-Ub with UIM-Rpn10 shows that both subunits of the heterodimer interact with the UIM of Rpn10, and in both cases the hydrophobic patch residues are involved (Figs. 6B, 6C, 6E, and 6F). The titration curves for both domains fit best to a 1:1 binding model, which suggests that either the Rub1 unit binds UIM much more weakly than Ub does or one molecule of UIM interacts with both the distal Rub1 and the proximal Ub. An average ^{15}N T_1 of 986 $\pm$ 141 ms (24 to 30 kDa) confirms the 1:1 stoichiometry of the UIM:Rub1-Ub complex (expected mass = 27 kDa). To measure the affinity, titration curves were analyzed yielding a K_d of 185 $\pm$ 103 μM for the distal Rub1 and of 36 $\pm$ 9 μM for the proximal Ub. Note that the latter K_d value is essentially the same as for monoUb binding to UIM-Rpn10 (66). Moreover, the ^{15}N T_1 values show a lesser increase for the distal Rub1 than for the proximal Ub (Table I), suggesting
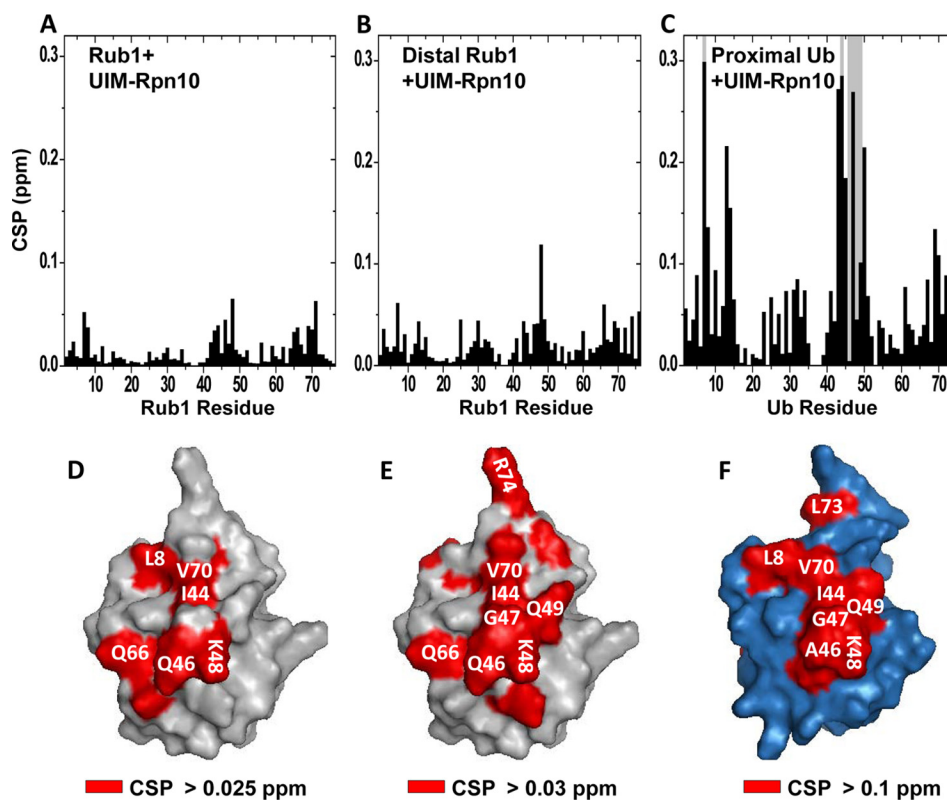
FIG. 6. **The Rub1-Ub heterodimer interacts with the UIM domain of Rpn10.** The upper panel shows the magnitude of CSPs (black bars) in backbone amides of either monomeric Rub1 (*A*) or the distal Rub1 (*B*) and proximal Ub (*C*) in the heterodimer upon addition of the UIM domain of Rpn10. The gray bars indicate residues exhibiting significant signal attenuations (>75%). The lower panel shows surface maps of the residues (marked in red) exhibiting significant perturbations (as indicated) and/or strong signal attenuations in either monoRub1 (*D*) or the distal Rub1 (*E*) and the proximal Ub (*F*) in the heterodimer caused by UIM-Rpn10.

that the UIM primarily binds to the latter. These results indicate that the UIM of Rpn10 interacts with the Rub1 unit in the heterodimer much more weakly than with the Ub unit.

The fact that Rub1 binds to the UIM and UBA domains from proteasomal and non-proteasomal Ub receptors raises the possibility that Rub1/Nedd8 is recognized by components of the Ub proteasome system essentially as Ub, and thus the possibility exists for competition between Rub1/Nedd8 and Ub for the same receptors. In order to address this issue, we performed a pulldown study in which we examined the ability of monomeric Rub1 (immobilized on beads) to pull out Ub receptors/shuttles directly from the whole cell extract. We used Rub1-deficient yeast cells (Δ*rub1*) to focus on competition between the slew of polyUb conjugates in extract and immobilized Rub1. As positive and negative controls, we used Ub beads and mock beads, respectively. The results (Fig. 7) clearly show that despite the presence of Ub and abundant polyUb conjugates in the whole cell extract, which were potentially competing with immobilized monomeric Rub1, this lonely Rub1 was able to pull down at least two known Ub receptors, Rpn10 and Dsk2. Both Rpn10 and Dsk2 were somewhat more labile on Rub1 than on Ub and washed off at high-salt washes, reflecting some hydrophilic nature of their association; however, a significant portion remained and was
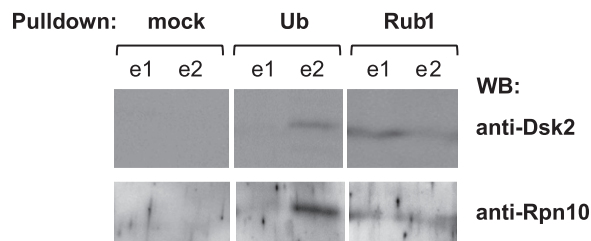

FIG. 7. **Rub1 can stably associate with known Ub receptors/ shuttles directly in whole cell extract and in competition with Ub.** His$_6$-Rub1 or His$_6$-Ub, immobilized on CH Sepharose 4B beads (150 μl), was incubated overnight at 4 °C with 2 ml of whole cell extract prepared from natively lysed Rub1-deficient yeast cells (Δ*rub1*). The beads were washed with lysis buffer followed by elutions with hydrophilic buffer or hydrophobic buffer. Hydrophilic and hydrophobic eluates (e1 and e2, respectively) were separated by means of SDS-PAGE and immunoblotted against Rpn10 and Dsk2. Mock beads were used as a negative control.

eluted only with stringent washes just like those that were bound to Ub.

Given the interactions observed for the Rub1-Ub heterodimer with both the proteasomal and the non-proteasomal receptors/shuttles, we focused our attention on testing whether this heterodimer is targeted and processed by the proteasome. Proteasomes are efficient deubiquitinases with
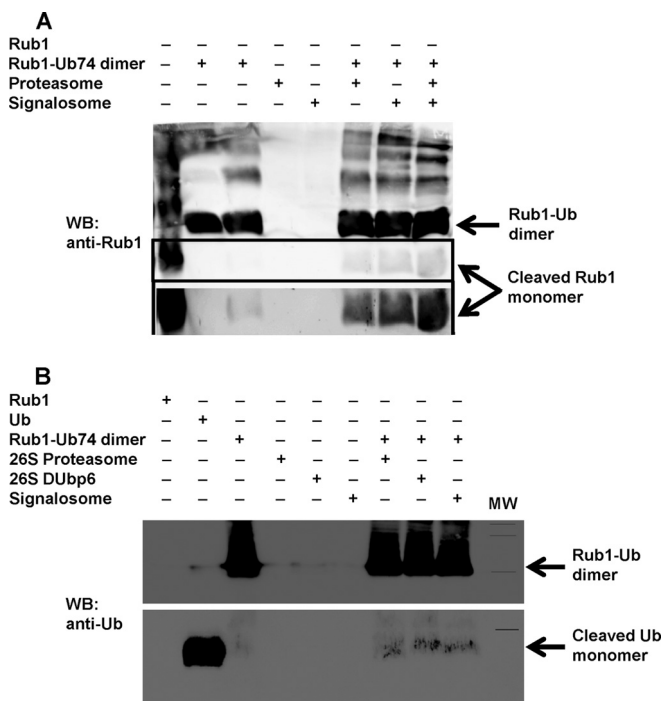
FIG. 8. **Cleavage of the Rub1-Ub heterodimer by both the 26S proteasome and the signalosome.** *A*, *in vitro* synthesized K48-linked Rub1-Ub heterodimer was incubated with either the 26S proteasome or the COP9 signalosome purified from yeast in a cleavage reaction at 30 °C overnight (12 to 16 h) followed by quenching upon the addition of 1X SDS loading buffer. The mixture was separated on SDS-PAGE followed by Western blot with anti-Rub1 antibody. The membrane was generated with two different exposure times: short exposure (shown in the rectangular box) and long exposure (shown in the open box). The running positions of the Rub1-Ub dimer and the Rub1 monomer are indicated by arrows. *B*, similar assay as in *A* but also including cleavage by the proteasome purified from a Ubp6-deficient strain (Δubp6) and blotted with anti-Ub antibody.

broad specificity (96–98); but how would they deal with Rub1? For this, *in vitro* synthesized Rub1-Ub heterodimer was incubated with affinity purified 26S proteasome from yeast cells. The reaction was quenched by adding SDS-loading buffer followed by SDS-PAGE separation and blotted with anti-Rub1 or anti-Ub antibody. Interestingly, we observed the presence of a significant amount of monoRub1 and monoUb in the lane where both the Rub1-Ub heterodimer and the proteasome were added, but not in the lanes where either the heterodimer or the proteasome was added separately (Fig. 8). This indicates that the purified yeast proteasome cleaves Rub1-Ub dimers into monomeric Rub1 and Ub. To rule out a possible role of Ubp6 in this process, we performed a similar cleavage assay with the proteasome purified from a Ubp6-deficient strain (Δubp6). The results (Fig. 8*B*) show that the WT and ΔUbp6 proteasomes behave essentially identically in the disassembly of Rub1-Ub heterodimers. A reasonable conclusion points to Rpn11 as the culprit responsible for the observed derubylase activity of the 26S proteasome.

In contrast to the proteasomes, COP9 signalosomes (CSN) are efficient derubylases, shown to cleave Rub1 from its conjugated substrate (99–102). In order to assess how CSN treats a mixed Rub1-Ub signal, we tested the ability of affinity purified yeast CSN to cleave the Rub1-Ub heterodimer. Indeed, isolated CSN was able to cleave the heterodimer into its monomeric subunits (Fig. 8). To summarize, the above findings indicate that the Rub1-Ub heterodimers not only are recognized and processed by the proteins involved in the Ub-proteasome pathway, but also are recognized and cleaved by the proteasome and by the signalosome.

DISCUSSION

Rub1/Nedd8 is the closest protein to Ub among all UBLs. However, their biological functions are very different. Whereas Ub modifies a broad spectrum of targets leading to a variety of outcomes such as intracellular sorting or proteasome-dependent degradation, the known targets of Rub1 for which there is a clear biological outcome are limited to a handful. Though Rub1 is structurally very similar to Ub, the attachment of Rub1 alters only protein function (in the case of cullins) and, to date, is not known to target for proteasomal degradation. In order to understand how the UBA domains of shuttle proteins differentiate between Ub and Rub1, we evaluated the interactions of Rub1 with the UBA domains of the known UBL-UBA proteins. Our NMR titration data show that Rub1 interacts with the UBA domains of all the shuttle proteins tested. The affinity of UBA-UQ1 and UBA-Ddi1 for Rub1 is very similar to the reported affinity of these UBA domains for Ub. However, UBA2-hHR23a binds Rub1 with an affinity ca. 4- to 5-fold higher than the affinity for Ub. Moreover, all these interactions involve the same surface of Rub1, which includes an entirely conserved hydrophobic patch and is very similar to the surface of Ub shown to interact with these UBA domains. This suggests that the UBA domains of these shuttle proteins do not differentiate between Ub and Rub1 and suggests a possible role of Rub1 in signaling proteasomal targeting, to either augment or possibly compete with degradation. This, along with the fact that at least tetramers of Ub increase affinity for some receptors, suggests that doping Rub1 into heterologous chains with Ub might alter the targeting hierarchy. Indeed, our mammalian transfection data show that Nedd8 forms a heterologous chain with Ub in which Nedd8 acts as a chain terminator. Although these heterologous chains were substrate free, they might be due to the cleavage of longer chains shaven off of targets catalyzed by the presence of numerous cellular isopeptidases, or they might be in the process of being built up (presumably by a class of E2 enzymes, such as E2–25K, Ubc13/Mms2, or Ube2s) and conjugated to their natural substrates, or both. Indeed, our data from this study (see Fig. 3*A* and supplemental Fig. S2), along with a recently published report (40), suggest the presence of several targets in cells that can be modified by these heterologous chains.

Our *in vitro* data show that the heterologous Rub1-Ub chains are readily formed using the E1 and E2 enzymes of the Ub pathway. However, these chains were not formed efficiently when we used the E1 of Rub1 in our *in vitro* experiments. This indicates that the enzymes of the Rub1 pathway show higher fidelity to the cognate UBL than the enzymes of the Ub pathway. Indeed, recent biochemical and crystallographic studies show that the E1 of Rub1 not only has a gating mechanism to prevent the misactivation of Ub, but also uniquely interacts with its cognate E2 to optimally conjugate Rub1 to its substrate (103–105). Similarly, the E1 of Ub also differentiates between these two UBLs to some extent (19). A study by the late Cecile Pickart and co-workers suggests that the E1 of Ub activates Rub1 *in vitro*, though with an efficiency about 100 times less than the efficiency of activation of Ub, and vice versa (19). Similarly, another report shows that lowering the Ub level by a mere 3.6-fold in U2OS cells triggers the conjugation of Rub1 to many substrates using the E1 enzyme of the Ub pathway (106). That report further states that U2OS cells contain free forms of Ub and Nedd8 in a roughly equimolar amount, so a 3.6-fold decrease in the free Ub concentration will increase the ratio of [Nedd8]:[Ub] from 1:1 to 3.6:1, and this is sufficient to trigger Ub E1-mediated neddylation in these cells. Although it requires further experimental verification, this indicates that our Nedd8-Ub heterologous chain possibly was synthesized in the cells also using the E1 enzyme of the Ub pathway.

We and others have previously shown that a tetraUb chain binds to the UBA domains much more tightly than a diUb, and a diUb binds much more tightly than monoUb (58–61, 66). Our titration data show that the UBA domains of Ub shuttle proteins bind the K48-linked Rub1-Ub heterodimer somewhat more tightly than they bind monomeric Rub1, which is by and large comparable to how the UBA domains of these shuttle proteins interact with diUb (see Table II and Figs. 2 and 5). This suggests that the shuttle proteins possibly bind a heterologous chain composed of three molecules of Ub and one distal molecule of Rub1 with an affinity comparable to that in their interaction with the tetramer of Ub.

Our data show that monoRub1 and the distal Rub1 in the Rub1-Ub heterodimer interact weakly with the UIM domain of Rpn10. This might be why Rub1-modified proteins are poor substrates for proteasomal degradation. However, the presence of Ub in the heterodimer significantly increases its affinity for the UIM domain (Table II), and this possibly explains why we see cleavage of the heterodimer into its monomeric subunits upon incubation with the proteasome. This suggests that a heterologous chain composed of at least a heterotetramer might function as an efficient degradation signal. Furthermore, our *in vitro* data show that these heterodimers are also cleaved by the COP9 signalosome, which indicates that a concerted effort by the proteasome and the signalosome might be required in order to process these heterologous chains within cells. Taken together, our data suggest reopen-

ing the question of whether Rub1 might target conjugates to the proteasome, especially in cases when it caps long polyUb chains or is found on targets that are simultaneously ubiquitinated on other residues.

The ability of the proteasome to remove the distal Rub1 from its Ub conjugate is unexpected, as a derubylation function implies the ability to recognize and process the Rub1 signal. Identification of the responsible subunits or components will require further investigation. Nevertheless, this previously undocumented enzymatic function of the proteasome expands the repertoire of its catalytic activities. That said, in order for mixed Rub1-Ub chains to serve as efficient proteasome targeting signals, they would be expected to be stable enough to survive disassembly by proteases for Ub or UBL domains. As we demonstrate in supplemental Fig. S6, one extremely fast and broad-based deubiquitinase (DUB), Usp2, is essentially inert toward Rub1-containing chains. Previously, a similar conclusion was reached based on the inability of a Nedd8 suicide inhibitor to effectively inhibit another Ub-specific protease, Usp21 (107). A possible consequence would be that under perturbation or certain induced stresses, Rub1-capped Ub chains (even ones shorter than typical chains) might be more resilient to disassembly by DUBs and thus promote targeting to CSN or proteasome, where metaloproteases of the MPN+/JAMM family readily process them.

The standing observation that Rub1 does not appear to promote degradation might be more an issue of bio-availability and the preference of the ubiquitination machinery for Ub over Rub1. However, in cases when Rub1 is activated by UBA1 (the E1 of Ub) and channeled into chains or polymeric modifications of widespread targets, our data suggest that it might very well behave rather similarly to Ub. Indeed, a recent report shows that a cullin called RTT101 can be rubylated or ubiquitinated on the same lysine residue and that in either case the outcome in terms of function is the same (108). Similarly, ubiquitination or rubylation sites of EGFR are shared, and in both cases the function is to internalize the activated receptor (35). This raises many questions as to why cells maintain the targets of two small proteins separately and how they are maintained as separate modifications. Several recent reports show that this is primarily due to the presence of selective E1s that are able to distinguish between them in normal cells (19, 109). However, under stress conditions, Rub1 can be cross-activated and conjugated to the Ub targets, and once on the target, the extreme similarities of Rub1 and Ub would allow them to form heterologous chains which then would be recognized by the shuttles and processed by the proteasome.

The current results provide mechanistic insights into how Rub1 may enter the "ubiquitin sphere of modification." As a consequence, a portion of rubylated/neddylated targets might not be specific substrates of Rub1/Nedd8 modification *per se*, but targets of heterologous chains, thus potentially affecting data obtained via affinity purification or Rub1/Nedd8 pull-outs.
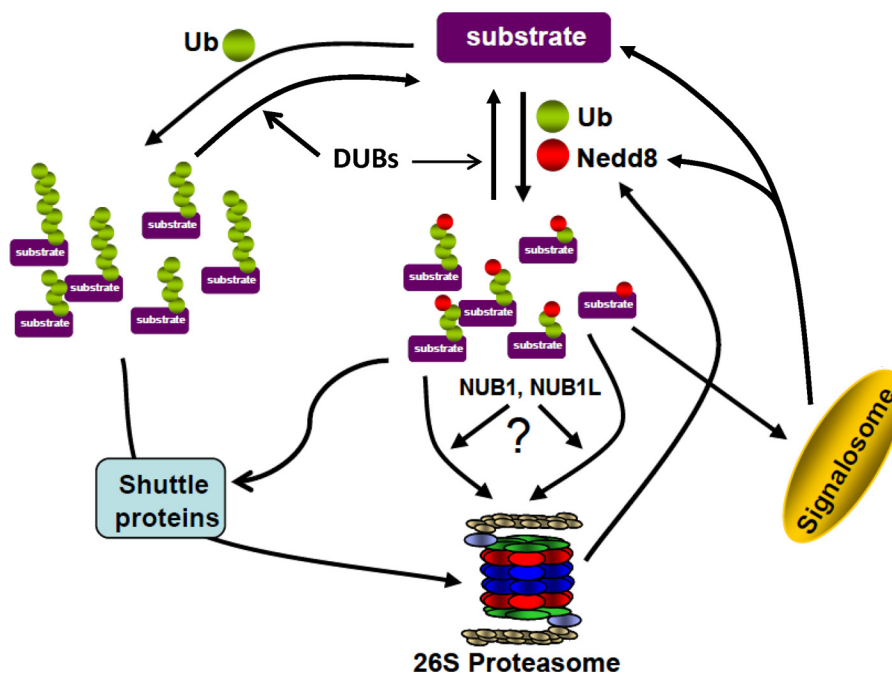
FIG. 9. **A model predicting the role of heterologous chains within cells.** Ub can form a very long chain on its substrate. Normally, this is not a problem for the cells. However, in certain conditions in which the free-Ub level in the cells is decreased (as conceived in the case of Alzheimer's and Parkinson's diseases), a change in the ratio of free Ub to Nedd8 triggers the activation of both Nedd8 and Ub by the enzymes of the Ub pathway. This leads to the formation of substantially shorter Ub chains on the substrate due to the chain-terminating ability of Nedd8. The formation of the heterologous chains replicates the function of Ub chains and at the same time helps avoid further depletion of free Ub in the cells. Our data indicate that these heterologous chains are processed by both the 26S proteasome and the COP9 signalosome, which suggests that these heterologous chains do not accumulate in the cells and instead are cleaved and subsequently recycled. Although we showed that the heterologous chains are recognized by the Ub binding domains of the Ub receptors, we do not exclude the possibility that these chains are also recognized by the dedicated Nedd8 receptors in the cells (for example, NUB1 and NUB1L).

Overall, our data suggest that there is not much to distinguish between Rub1 and Ub, and once Rub1 is channeled into the Ub pathway, Rub1 or Rub1-Ub heterologous chains are recognized and processed pretty much like Ub or Ub chains. This raises a question about why the cell machineries would synthesize two different types of chains to perform the same function. An obvious explanation is provided by our observation that Rub1 acts as a chain terminator. We present here an attractive but purely speculative model (Fig. 9) in which the heterologous chains formed by the enzymes of the Ub pathway are shorter and synthesized efficiently when the level of free Ub is depleted. This could be advantageous for the cells in conditions when they need to conserve a certain level of free Ub. For example, it has been shown that Ub conjugates are accumulated in many neurodegenerative diseases, including Alzheimer's and Parkinson's (110–112). The condition in these cells could lead to the depletion of free Ub, which might trigger the synthesis of the heterologous chains. Indeed, Nedd8 has been shown to be present in protein aggregates in these neurodegenerative diseases (113). The formation of the heterologous chains replicates the function of Ub chains and at the same time ensures avoidance of the further depletion of free Ub within cells. This might also occur upon over-expression of Nedd8. It would be interesting to

chart conditions or cellular compartments for which the Nedd8/Ub ratio naturally increases. Our finding that the heterologous chains are cleaved by both the proteasome and the signalosome suggests that these chains could be processed and recycled, which would be necessary in order to avoid the accumulation and subsequent toxic effect, if any, of heterologous chains within cells. It would be difficult, although not impossible, to show this within cells, but the data presented here are consistent with this model.

** To whom correspondence should be addressed: David Fushman, E-mail: fushman@umd.edu; Michael H. Glickman, E-mail: glickman@technix.technion.ac.il.

REFERENCES

1. Vodermaier, H. C. (2004) APC/C and SCF: controlling each other and the cell cycle. *Curr. Biol.* **14,** R787-R796

2. Dornan, D., Wertz, I., Shimizu, H., Arnott, D., Frantz, G. D., Dowd, P., O'Rourke, K., Koeppen, H., and Dixit, V. M. (2004) The ubiquitin ligase COP1 is a critical negative regulator of p53. *Nature* **429,** 86–92

3. Wang, Y., Werz, C., Xu, D., Chen, Z., Li, Y., Hafen, E., and Bergmann, A. (2008) Drosophila cbl is essential for control of cell death and cell differentiation during eye development. *PLoS One* **3,** e1447

4. Ou, C. Y., Pi, H., and Chien, C. T. (2003) Control of protein degradation by E3 ubiquitin ligases in Drosophila eye development. *Trends Genet*. **19,** 382–389

5. Conaway, R. C., Brower, C. S., and Conaway, J. W. (2002) Emerging roles of ubiquitin in transcription regulation. *Science* **296,** 1254–1258

6. Clague, M. J., and Urbé, S. (2010) Ubiquitin: same molecule, different degradation pathways. *Cell* **143,** 682–685

7. Hershko, A., and Ciechanover, A. (1998) The ubiquitin system. *Annu. Rev. Biochem.* **67,** 425–479

8. Hochstrasser, M. (1996) Ubiquitin-dependent protein degradation. *Annu. Rev. Genet.* **30,** 405–439

9. Hochstrasser, M. (2006) Lingering mysteries of ubiquitin-chain assembly. *Cell* **124,** 27–34

10. Kerscher, O., Felberbaum, R., and Hochstrasser, M. (2006) Modification of proteins by ubiquitin and ubiquitin-like proteins. *Annu. Rev. Cell Dev. Biol.* **22,** 159–180

11. Pickart, C. M. (2004) Back to the future with ubiquitin. *Cell* **116,** 181–190

12. Eddins, M. J., Varadan, R., Fushman, D., Pickart, C. M., and Wolberger, C. (2007) Crystal structure and solution NMR studies of Lys48-linked tetraubiquitin at neutral pH. *J. Mol. Biol.* **367,** 204–211

13. Varadan, R., Walker, O., Pickart, C., and Fushman, D. (2002) Structural properties of polyubiquitin chains in solution. *J. Mol. Biol.* **324,** 637–647

14. Varadan, R., Assfalg, M., Haririnia, A., Raasi, S., Pickart, C., and Fushman, D. (2004) Solution conformation of Lys63-linked di-ubiquitin chain provides clues to functional diversity of polyubiquitin signaling. *J. Biol. Chem.* **279,** 7055–7063

15. Beau, I., Esclatine, A., and Codogno, P. (2008) Lost to translation: when autophagy targets mature ribosomes. *Trends Cell Biol.* **18,** 311–314

16. Lundgren, K., Montes de Oca Luna, R., McNeill, Y. B., Emerick, E. P., Spencer, B., Barfield, C. R., Lozano, G., Rosenberg, M. P., and Finlay, C. A. (1997) Targeted expression of MDM2 uncouples S phase from mitosis and inhibits mammary gland development independent of p53. *Genes Dev.* **11,** 714–725

17. Hofmann, R. M., and Pickart, C. M. (1999) Noncanonical MMS2-encoded ubiquitin-conjugating enzyme functions in assembly of novel polyubiquitin chains for DNA repair. *Cell* **96,** 645–653

18. Ulrich, H. D. (2007) Conservation of DNA damage tolerance pathways from yeast to humans. *Biochem. Soc. Trans.* **35,** 1334–1337

19. Whitby, F. G., Xia, G., Pickart, C. M., and Hill, C. P. (1998) Crystal structure of the human ubiquitin-like protein NEDD8 and interactions with ubiquitin pathway enzymes. *J. Biol. Chem.* **273,** 34983–34991

20. Choi, Y. S., Jeon, Y. H., Ryu, K. S., and Cheong, C. (2009) 60th residues of ubiquitin and Nedd8 are located out of E2-binding surfaces, but are important for K48 ubiquitin-linkage. *FEBS Lett.* **583,** 3323–3328

21. Rao-Naik, C., delaCruz, W., Laplaza, J. M., Tan, S., Callis, J., and Fisher, A. J. (1998) The rub family of ubiquitin-like proteins. Crystal structure of Arabidopsis rub1 and expression of multiple rubs in Arabidopsis. *J. Biol. Chem.* **273,** 34976–34982

22. Hochstrasser, M. (2000) Biochemistry. All in the ubiquitin family. *Science* **289,** 563–564

23. Liakopoulos, D., Doenges, G., Matuschewski, K., and Jentsch, S. (1998) A novel protein modification pathway related to the ubiquitin system. *EMBO J.* **17,** 2208–2214

24. Huang, D. T., Miller, D. W., Mathew, R., Cassell, R., Holton, J. M., Roussel, M. F., and Schulman, B. A. (2004) A unique E1-E2 interaction required for optimal conjugation of the ubiquitin-like protein NEDD8. *Nat. Struct. Mol. Biol.* **11,** 927–935

25. Huang, D. T., Paydar, A., Zhuang, M., Waddell, M. B., Holton, J. M., and Schulman, B. A. (2005) Structural basis for recruitment of Ubc12 by an E2 binding domain in NEDD8's E1. *Mol. Cell* **17,** 341–350

26. Hori, T., Osaka, F., Chiba, T., Miyamoto, C., Okabayashi, K., Shimbara, N., Kato, S., and Tanaka, K. (1999) Covalent modification of all members of human cullin family proteins by NEDD8. *Oncogene* **18,** 6829–6834

27. Rabut, G., and Peter, M. (2008) Function and regulation of protein neddylation. 'Protein modifications: beyond the usual suspects' review series. *EMBO Rep.* **9,** 969–976

28. Merlet, J., Burger, J., Gomes, J. E., and Pintard, L. (2009) Regulation of cullin-RING E3 ubiquitin-ligases by neddylation and dimerization. *Cell Mol. Life Sci.* **66,** 1924–1938

29. Harper, J. (2004) Neddylating the guardian; Mdm2 catalyzed conjugation of Nedd8 to p53. *Cell* **118,** 2–4

30. Xirodimas, D. P., Saville, M. K., Bourdon, J. C., Hay, R. T., and Lane, D. P. (2004) Mdm2-mediated NEDD8 conjugation of p53 inhibits its transcriptional activity. *Cell* **118,** 83–97

31. Abida, W. M., Nikolaev, A., Zhao, W., Zhang, W., and Gu, W. (2007) FBXO11 promotes the Neddylation of p53 and inhibits its transcriptional activity. *J. Biol. Chem.* **282,** 1797–1804

32. Watson, I. R., Blanch, A., Lin, D. C., Ohh, M., and Irwin, M. S. (2006) Mdm2-mediated NEDD8 modification of TAp73 regulates its transactivation function. *J. Biol. Chem.* **281,** 34096–34103

33. Xirodimas, D. P., Sundqvist, A., Nakamura, A., Shen, L., Botting, C., and Hay, R. T. (2008) Ribosomal proteins are targets for the NEDD8 pathway. *EMBO Rep.* **9,** 280–286

34. Sundqvist, A., Liu, G., Mirsaliotis, A., and Xirodimas, D. P. (2009) Regulation of nucleolar signalling to p53 through NEDDylation of L11. *EMBO Rep.* **10,** 1132–1139

35. Oved, S., Mosesson, Y., Zwang, Y., Santonico, E., Shtiegman, K., Marmor, M. D., Kochupurakkal, B. S., Katz, M., Lavi, S., Cesareni, G., and Yarden, Y. (2006) Conjugation to Nedd8 instigates ubiquitylation and down-regulation of activated receptor tyrosine kinases. *J. Biol. Chem.* **281,** 21640–21651

36. Broemer, M., Tenev, T., Rigbolt, K. T., Hempel, S., Blagoev, B., Silke, J., Ditzel, M., and Meier, P. (2010) Systematic in vivo RNAi analysis identifies IAPs as NEDD8-E3 ligases. *Mol. Cell* **40,** 810–822

37. Benjamin, S., and Steller, H. (2010) Another tier for caspase regulation: IAPs as NEDD8 E3 ligases. *Dev. Cell* **19,** 791–792

38. Um, J. W., Han, K. A., Im, E., Oh, Y., Lee, K., and Chung, K. C. (2012) Neddylation positively regulates the ubiquitin E3 ligase activity of parkin. *J. Neurosci. Res.* **90,** 1030–1042

39. Choo, Y. S., Vogler, G., Wang, D., Kalvakuri, S., Iliuk, A., Tao, W. A., Bodmer, R., and Zhang, Z. (2012) Regulation of parkin and PINK1 by neddylation. *Hum. Mol. Genet.* **21,** 2514–2523

40. Leidecker, O., Matic, I., Mahata, B., Pion, E., and Xirodimas, D. P. (2012) The ubiquitin E1 enzyme Ube1 mediates NEDD8 activation under diverse stress conditions. *Cell Cycle* **11,** 1142–1150

41. Lane, D. P. (2012) Stress, specificity and the NEDD8 proteome. *Cell Cycle* **11,** 1488–1489

42. Rosenzweig, R., Bronner, V., Zhang, D., Fushman, D., and Glickman, M. H. (2012) Rpn1 and rpn2 coordinate ubiquitin processing factors at proteasome. *J. Biol. Chem.* **287,** 14659–14671

43. Singh, R. K., Iyappan, S., and Scheffner, M. (2007) Hetero-oligomerization with MdmX rescues the ubiquitin/Nedd8 ligase activity of RING finger mutants of Mdm2. *J. Biol. Chem.* **282,** 10901–10907

44. Cornilescu, G., Delaglio, F., and Bax, A. (1999) Protein backbone angle restraints from searching a database for chemical shift and sequence homology. *J. Biomol. NMR* **13,** 289–302

45. Shen, Y., Lange, O., Delaglio, F., Rossi, P., Aramini, J. M., Liu, G., Eletsky, A., Wu, Y., Singarapu, K. K., Lemak, A., Ignatchenko, A., Arrowsmith, C. H., Szyperski, T., Montelione, G. T., Baker, D., and Bax, A. (2008) Consistent blind protein structure generation from NMR chemical shift data. *Proc. Natl. Acad. Sci. U.S.A.* **105,** 4685–4690

46. Shen, Y., Bryan, P. N., He, Y., Orban, J., Baker, D., and Bax, A. (2010) De novo structure generation using chemical shifts for proteins with high-sequence identity but different folds. *Protein Sci*. **19,** 349–356

47. Schauber, C., Chen, L., Tongaonkar, P., Vega, I., Lambertson, D., Potts, W., and Madura, K. (1998) Rad23 links DNA repair to the ubiquitin/proteasome pathway. *Nature* **391,** 715–718

48. Ortolan, T. G., Tongaonkar, P., Lambertson, D., Chen, L., Schauber, C., and Madura, K. (2000) The DNA repair protein rad23 is a negative

regulator of multi-ubiquitin chain assembly. *Nat. Cell Biol.* **2,** 601–608

49. Kleijnen, M. F., Shih, A. H., Zhou, P., Kumar, S., Soccio, R. E., Kedersha, N. L., Gill, G., and Howley, P. M. (2000) The hPLIC proteins may provide a link between the ubiquitination machinery and the proteasome. *Mol. Cell* **6,** 409–419

50. Kaplun, L., Tzirkin, R., Bakhrat, A., Shabek, N., Ivantsiv, Y., and Raveh, D. (2005) The DNA damage-inducible UbL-UbA protein Ddi1 participates in Mec1-mediated degradation of Ho endonuclease. *Mol. Cell Biol.* **25,** 5355–5362

51. Ivantsiv, Y., Kaplun, L., Tzirkin-Goldin, R., Shabek, N., and Raveh, D. (2006) Unique role for the UbL-UbA protein Ddi1 in turnover of SCFUfo1 complexes. *Mol. Cell. Biol.* **26,** 1579–1588

52. Elsasser, S., Gali, R. R., Schwickart, M., Larsen, C. N., Leggett, D. S., Müller, B., Feng, M. T., Tübing, F., Dittmar, G. A., and Finley, D. (2002) Proteasome subunit Rpn1 binds ubiquitin-like protein domains. *Nat. Cell Biol.* **4,** 725–730

53. Gomez, T. A., Kolawa, N., Gee, M., Sweredoski, M. J., and Deshaies, R. J. (2011) Identification of a functional docking site in the Rpn1 LRR domain for the UBA-UBL domain protein Ddi1. *BMC Biol.* **9,** 33

54. Kang, Y., Vossler, R. A., Diaz-Martinez, L. A., Winter, N. S., Clarke, D. J., and Walters, K. J. (2006) UBL/UBA ubiquitin receptor proteins bind a common tetraubiquitin chain. *J. Mol. Biol.* **356,** 1027–1035

55. Wilkinson, C. R., Seeger, M., Hartmann-Petersen, R., Stone, M., Wallace, M., Semple, C., and Gordon, C. (2001) Proteins containing the UBA domain are able to bind to multi-ubiquitin chains. *Nat. Cell Biol.* **3,** 939–943

56. Hartmann-Petersen, R., and Gordon, C. (2004) Protein degradation: recognition of ubiquitinylated substrates. *Curr. Biol.* **14,** R754-R756

57. Wang, X., and Huang, L. (2008) Identifying dynamic interactors of protein complexes by quantitative mass spectrometry. *Mol. Cell. Proteomics* **7,** 46–57

58. Varadan, R., Assfalg, M., Raasi, S., Pickart, C., and Fushman, D. (2005) Structural determinants for selective recognition of a Lys48-linked polyubiquitin chain by a UBA domain. *Mol. Cell* **18,** 687–698

59. Zhang, D., Raasi, S., and Fushman, D. (2008) Affinity makes the difference: nonselective interaction of the UBA domain of Ubiquilin-1 with monomeric ubiquitin and polyubiquitin chains. *J. Mol. Biol.* **377,** 162–180

60. Trempe, J. F., Brown, N. R., Lowe, E. D., Gordon, C., Campbell, I. D., Noble, M. E., and Endicott, J. A. (2005) Mechanism of Lys48-linked polyubiquitin chain recognition by the Mud1 UBA domain. *EMBO J.* **24,** 3178–3189

61. Raasi, S., Varadan, R., Fushman, D., and Pickart, C. M. (2005) Diverse polyubiquitin interaction properties of ubiquitin-associated domains. *Nat. Struct. Mol. Biol.* **12,** 708–714

62. Raasi, S., Orlov, I., Fleming, K. G., and Pickart, C. M. (2004) Binding of polyubiquitin chains to ubiquitin-associated (UBA) domains of HHR23A. *J. Mol. Biol.* **341,** 1367–1379

63. Wishart, D. S., and Sykes, B. D. (1994) Chemical shifts as a tool for structure determination. *Methods Enzymol.* **239,** 363–392

64. Oldfield, E. (1995) Chemical shifts and three-dimensional protein structures. *J. Biomol. NMR* **5,** 217–225

65. Zuiderweg, E. R. (2002) Mapping protein-protein interactions in solution by NMR spectroscopy. *Biochemistry* **41,** 1–7

66. Zhang, D., Chen, T., Ziv, I., Rosenzweig, R., Matiuhin, Y., Bronner, V., Glickman, M. H., and Fushman, D. (2009) Together, Rpn10 and Dsk2 can serve as a polyubiquitin chain-length sensor. *Mol. Cell* **36,** 1018–1033

67. Fielding, L. (2003) NMR methods for the determination of protein-ligand dissociation constants. *Curr. Top. Med. Chem.* **3,** 39–53

68. Clarkson, J., and Campbell, I. D. (2003) Studies of protein-ligand interactions by NMR. *Biochem. Soc. Trans.* **31,** 1006–1009

69. Bertolaet, B. L., Clarke, D. J., Wolff, M., Watson, M. H., Henze, M., Divita, G., and Reed, S. I. (2001) UBA domains of DNA damage-inducible proteins interact with ubiquitin. *Nat. Struct. Biol.* **8,** 417–422

70. Sims, J. J., Haririnia, A., Dickinson, B. C., Fushman, D., and Cohen, R. E. (2009) Avid interactions underlie the Lys63-linked polyubiquitin binding specificities observed for UBA domains. *Nat. Struct. Mol. Biol.* **16,** 883–889

71. Mueller, T. D., Kamionka, M., and Feigon, J. (2004) Specificity of the interaction between ubiquitin-associated domains and ubiquitin. *J. Biol. Chem.* **279,** 11926–11936

72. Ryu, K. S., Lee, K. J., Bae, S. H., Kim, B. K., Kim, K. A., and Choi, B. S. (2003) Binding surface mapping of intra- and interdomain interactions among hHR23B, ubiquitin, and polyubiquitin binding site 2 of S5a. *J. Biol. Chem.* **278,** 36621–36627

73. Mah, A. L., Perry, G., Smith, M. A., and Monteiro, M. J. (2000) Identification of ubiquilin, a novel presenilin interactor that increases presenilin protein accumulation. *J. Cell Biol.* **151,** 847–862

74. Ohno, A., Jee, J., Fujiwara, K., Tenno, T., Goda, N., Tochio, H., Kobayashi, H., Hiroaki, H., and Shirakawa, M. (2005) Structure of the UBA domain of Dsk2p in complex with ubiquitin molecular determinants for ubiquitin recognition. *Structure* **13,** 521–532

75. Jeram, S. M., Srikumar, T., Zhang, X. D., Anne Eisenhauer, H., Rogers, R., Pedrioli, P. G., Matunis, M., and Raught, B. (2010) An improved SUMmOn-based methodology for the identification of ubiquitin and ubiquitin-like protein conjugation sites identifies novel ubiquitin-like protein chain linkages. *Proteomics* **10,** 254–265

76. Ohki, Y., Funatsu, N., Konishi, N., and Chiba, T. (2009) The mechanism of poly-NEDD8 chain formation in vitro. *Biochem. Biophys. Res. Commun.* **381,** 443–447

77. Jones, J., Wu, K., Yang, Y., Guerrero, C., Nillegoda, N., Pan, Z. Q., and Huang, L. (2008) A targeted proteomic analysis of the ubiquitin-like modifier nedd8 and associated proteins. *J. Proteome Res.* **7,** 1274–1287

78. Goettsch, S., and Bayer, P. (2002) Structural attributes in the conjugation of ubiquitin, SUMO and RUB to protein substrates. *Front. Biosci.* **7,** a148-a162

79. Behrends, C., and Harper, J. W. (2011) Constructing and decoding unconventional ubiquitin chains. *Nat. Struct. Mol. Biol.* **18,** 520–528

80. Ikeda, F., and Dikic, I. (2008) Atypical ubiquitin chains: new molecular signals. 'Protein Modifications: Beyond the Usual Suspects' review series. *EMBO Rep.* **9,** 536–542

81. Ziv, I., Matiuhin, Y., Kirkpatrick, D. S., Erpapazoglou, Z., Leon, S., Pantazopoulou, M., Kim, W., Gygi, S. P., Haguenauer-Tsapis, R., Reis, N., Glickman, M. H., and Kleifeld, O. (2011) A perturbed ubiquitin landscape distinguishes between ubiquitin in trafficking and in proteolysis. *Mol. Cell. Proteomics* **10,** M111.009753

82. Chen, Z., and Pickart, C. M. (1990) A 25-kilodalton ubiquitin carrier protein (E2) catalyzes multi-ubiquitin chain synthesis via lysine 48 of ubiquitin. *J. Biol. Chem.* **265,** 21835–21842

83. Chen, Z. J., Niles, E. G., and Pickart, C. M. (1991) Isolation of a cDNA encoding a mammalian multiubiquitinating enzyme (E225K) and overexpression of the functional enzyme in *Escherichia coli*. *J. Biol. Chem.* **266,** 15698–15704

84. Hofmann, R. M., and Pickart, C. M. (2001) In vitro assembly and recognition of Lys-63 polyubiquitin chains. *J. Biol. Chem.* **276,** 27936–27943

85. VanDemark, A. P., Hofmann, R. M., Tsui, C., Pickart, C. M., and Wolberger, C. (2001) Molecular insights into polyubiquitin chain assembly: crystal structure of the Mms2/Ubc13 heterodimer. *Cell* **105,** 711–720

86. Schrader, E. K., Harstad, K. G., and Matouschek, A. (2009) Targeting proteins for degradation. *Nat. Chem. Biol.* **5,** 815–822

87. Jung, T., Catalgol, B., and Grune, T. (2009) The proteasomal system. *Mol. Aspects Med.* **30,** 191–296

88. Dantuma, N. P., Heinen, C., and Hoogstraten, D. (2009) The ubiquitin receptor Rad23: at the crossroads of nucleotide excision repair and proteasomal degradation. *DNA Repair (Amst.)* **8,** 449–460

89. Finley, D. (2009) Recognition and processing of ubiquitin-protein conjugates by the proteasome. *Annu. Rev. Biochem.* **78,** 477–513

90. Lai, M. Y., Zhang, D., Laronde-Leblanc, N., and Fushman, D. (2012) Structural and biochemical studies of the open state of Lys48-linked diubiquitin. *Biochim. Biophys. Acta* **1823,** 2046–2056

91. van Nocker, S., Sadis, S., Rubin, D. M., Glickman, M., Fu, H., Coux, O., Wefes, I., Finley, D., and Vierstra, R. D. (1996) The multiubiquitin-chain-binding protein Mcb1 is a component of the 26S proteasome in Saccharomyces cerevisiae and plays a nonessential, substrate-specific role in protein turnover. *Mol. Cell Biol.* **16,** 6020–6028

92. Husnjak, K., Elsasser, S., Zhang, N., Chen, X., Randles, L., Shi, Y., Hofmann, K., Walters, K. J., Finley, D., and Dikic, I. (2008) Proteasome subunit Rpn13 is a novel ubiquitin receptor. *Nature* **453,** 481–488

93. Lam, Y. A., Lawson, T. G., Velayutham, M., Zweier, J. L., and Pickart, C. M. (2002) A proteasomal ATPase subunit recognizes the polyubiquitin degradation signal. *Nature* **416,** 763–767

94. Besten, W., Verma, R., Kleiger, G., Oania, R. S., and Deshaies, R. J. (2012) NEDD8 links cullin-RING ubiquitin ligase function to the p97 pathway. *Nat. Struct. Mol. Biol.* **19,** 511–516

95. Bandau, S., Knebel, A., Gage, Z. O., Wood, N. T., and Alexandru, G. (2012) UBXN7 docks on neddylated cullin complexes using its UIM motif and causes HIF1α accumulation. *BMC Biol.* **10,** 36

96. Guterman, A., and Glickman, M. H. (2004) Complementary roles for Rpn11 and Ubp6 in deubiquitination and proteolysis by the proteasome. *J. Biol. Chem.* **279,** 1729–1738

97. Verma, R., and Deshaies, R. J. (2005) Assaying degradation and deubiquitination of a ubiquitinated substrate by purified 26S proteasomes. *Methods Enzymol.* **398,** 391–399

98. Lee, M. J., Lee, B. H., Hanna, J., King, R. W., and Finley, D. (2011) Trimming of ubiquitin chains by proteasome-associated deubiquitinating enzymes. *Mol. Cell. Proteomics* **10,** R110.003871

99. Yamoah, K., Wu, K., and Pan, Z. Q. (2005) In vitro cleavage of Nedd8 from cullin 1 by COP9 signalosome and deneddylase 1. *Methods Enzymol.* **398,** 509–522

100. Min, K. W., Kwon, M. J., Park, H. S., Park, Y., Yoon, S. K., and Yoon, J. B. (2005) CAND1 enhances deneddylation of CUL1 by COP9 signalosome. *Biochem. Biophys. Res. Commun.* **334,** 867–874

101. Lyapina, S., Cope, G., Shevchenko, A., Serino, G., Tsuge, T., Zhou, C., Wolf, D. A., Wei, N., and Deshaies, R. J. (2001) Promotion of NEDD-CUL1 conjugate cleavage by COP9 signalosome. *Science* **292,** 1382–1385

102. Yu, Z., Kleifeld, O., Lande-Atir, A., Bsoul, M., Kleiman, M., Krutauz, D., Book, A., Vierstra, R. D., Hofmann, K., Reis, N., Glickman, M. H., and Pick, E. (2011) Dual function of Rpn5 in two PCI complexes, the 26S proteasome and COP9 signalosome. *Mol. Biol. Cell* **22,** 911–920

103. Huang, D. T., Hunt, H. W., Zhuang, M., Ohi, M. D., Holton, J. M., and Schulman, B. A. (2007) Basis for a ubiquitin-like protein thioester switch toggling E1-E2 affinity. *Nature* **445,** 394–398

104. Huang, D. T., Zhuang, M., Ayrault, O., and Schulman, B. A. (2008) Identification of conjugation specificity determinants unmasks vestigial preference for ubiquitin within the NEDD8 E2. *Nat. Struct. Mol. Biol.* **15,** 280–287

105. Souphron, J., Waddell, M. B., Paydar, A., Tokgöz-Gromley, Z., Roussel, M. F., and Schulman, B. A. (2008) Structural dissection of a gating mechanism preventing misactivation of ubiquitin by NEDD8's E1. *Biochemistry* **47,** 8961–8969

106. Hjerpe, R., Thomas, Y., Chen, J., Zemla, A., Curran, S., Shpiro, N., Dick, L. R., and Kurz, T. (2011) Changes in the ratio of free Nedd8 to ubiquitin triggers neddylation by ubiquitin enzymes. *Biochem. J.* **441,** 927–936

107. Ye, Y., Akutsu, M., Reyes-Turcu, F., Enchev, R. I., Wilkinson, K. D., and Komander, D. (2011) Polyubiquitin binding and cross-reactivity in the USP domain deubiquitinase USP21. *EMBO Rep.* **12,** 350–357

108. Rabut, G., Le Dez, G., Verma, R., Makhnevych, T., Knebel, A., Kurz, T., Boone, C., Deshaies, R. J., and Peter, M. (2011) The TFIIH subunit Tfb3 regulates cullin neddylation. *Mol. Cell* **43,** 488–495

109. Walden, H., Podgorski, M. S., Huang, D. T., Miller, D. W., Howard, R. J., Minor, D. L., Holton, J. M., and Schulman, B. A. (2003) The structure of the APPBP1-UBA3-NEDD8-ATP complex reveals the basis for selective ubiquitin-like protein activation by an E1. *Mol. Cell* **12,** 1427–1437

110. Dammer, E. B., Na, C. H., Xu, P., Seyfried, N. T., Duong, D. M., Cheng, D., Gearing, M., Rees, H., Lah, J. J., Levey, A. I., Rush, J., and Peng, J. (2011) Polyubiquitin linkage profiles in three models of proteolytic stress suggest the etiology of Alzheimer disease. *J. Biol. Chem.* **286,** 10457–10465

111. Lam, Y. A., Pickart, C. M., Alban, A., Landon, M., Jamieson, C., Ramage, R., Mayer, R. J., and Layfield, R. (2000) Inhibition of the ubiquitin-proteasome system in Alzheimer's disease. *Proc. Natl. Acad. Sci. U.S.A.* **97,** 9902–9906

112. Tanaka, K., Suzuki, T., Chiba, T., Shimura, H., Hattori, N., and Mizuno, Y. (2001) Parkin is linked to the ubiquitin pathway. *J. Mol. Med. (Berl.)* **79,** 482–494

113. Mori, F., Nishie, M., Piao, Y. S., Kito, K., Kamitani, T., Takahashi, H., and Wakabayashi, K. (2005) Accumulation of NEDD8 in neuronal and glial inclusions of neurodegenerative disorders. *Neuropathol. Appl. Neurobiol.* **31,** 53–61